Pradhan and Das
Protection and Control of Modern Power Systems (2023) 8:49
https://doi.org/10.1186/s41601-023-00322-w

Protection and Control of
Modern Power Systems

ORIGINAL RESEARCH

Open Access

Sliding mode controller design via delay-dependent H_∞ stabilization criterion for load frequency regulation

Subrat Kumar Pradhan[1] and Dushmanta Kumar Das[2*]

Abstract

This work presents a control approach based on sliding-mode-control (SMC) to design robust H_∞ state feedback controllers for load frequency regulation of delayed interconnected power system (IPS) with parametric uncertainties. Considering both state feedback control strategy and delayed feedback control strategy, two SMC laws are proposed. The proposed control laws are designed to improve the stability and disturbance rejection performance of delayed IPS, while stabilization criteria in the form of linear matrix inequality are derived by choosing a Lyapunov–Krasovskii functional. An artificial time-delay is incorporated in the control law design of the delayed feedback control structure to enhance the controller performance. A numerical example is considered to study the control performance of the proposed controllers and simulation results are provided to observe the dynamic response of the IPS.

Keywords Sliding mode control, Delay-dependent stabilization, H_∞ performance, Time-delay, Load frequency control

1 Introduction

Stable power system operation needs stability in frequency because frequency reflects the status of the real power balance between power supply and load demand [1, 2]. Alternators and other power devices deviate from stable operating condition due to fluctuation in frequency, which can lead to unstable and unsafe operation of the entire power system [3, 4]. Disturbance in load demand is the main cause of originating frequency and voltage oscillations in power system [5, 6]. Therefore, load frequency control (LFC) is an essential need of power system for its smooth operation [7, 8]. Using modern technologies, simple power system areas are interconnected through tie-lines to create an interconnected power system (IPS) [9, 10]. The main objective of a well designed IPS is to regulate frequency variation within tolerable limits during abnormal condition of IPS operation, i.e., load variation or sudden change in load demand [6, 11, 12].

In the last few decades, many traditional control techniques have been proposed to solve LFC problem in power system. Proportional-Integral (PI) control method [13] is first proposed to solve LFC problem, while decentralized robust PI controller based on Kharitonov's theorem is designed for LFC of a multi-area IPS in [14]. Various control schemes are designed for solving LFC problem of uncertain IPS, such as robust control scheme based on Riccati-equation [15] and adaptive control scheme with system parameter variation [16]. An active disturbance rejection control approach is proposed to develop a robust decentralized LFC algorithm for a three-area IPS in [17], while in [18], pole-placement method based variable structure controller is proposed for LFC of IPS.

*Correspondence:
Dushmanta Kumar Das
dushmantakumardas29@gmail.com
[1] Department of Electrical Engineering, Indira Gandhi Institute of Technology, Sarang, Dhenkanal 759146, India
[2] Department of Electrical and Electronics Engineering, National Institute of Technology Nagaland, Dimapur 797103, India

A finite time is always needed to measure control signals, compute control action and actuate the plant. This finite time requirement in every closed-loop system is termed as time-delay. Stability of closed-loop systems is affected by this delay because of its destabilizing nature [8]. Time-delay appears in IPS due to two main reasons, i.e.: (i) time needed for frequency and tie-line power measurement; and (ii) time taken in signal transmission from the remote terminal unit to the control centre and from the control centre to the generating unit [19]. Presence of time-delay in IPS sometimes leads to system instability and performance degradation [20, 21]. Therefore, time-delay should be included properly in LFC design of IPS to solve frequency deviation problem. Different control schemes have been used to design controllers for solving the LFC problem of time-delayed IPS. A decentralized robust PI controller is designed for LFC of power system with delay in [22], while state feedback control strategy based on linear matrix inequality (LMI) is adopted for LFC of IPS with delay in [23]. An iterative LMI based robust LFC algorithm is developed in [24] for time-delay IPS, while Lyapunov theory based delay-dependent stability criterion is developed in [25] for LFC by considering constant delay and time-varying delay in IPS. In [26], a delay-dependent robust PID-type controller is designed to regulate frequency of a three-area IPS with communication delay. Considering the existence of time-delay in the local PI-type LFC signals of an IPS, delay-dependent stability criteria are developed for the delayed LFC scheme in [27]. Although the above mentioned literatures based on delayed LFC design have well considered the effect of time-delay in LFC scheme, no specific method has been implemented to improve the performance of LFC scheme which is degraded due to the existence of time-delay.

Stabilizing nature of time-delay in system dynamics is an interesting aspect studied in [28, 29]. A finite valued known time-delay is introduced intentionally in the control law design to improve the stability of a delayed system in [8]. A few research results are available in literatures where time-delay is introduced in control design for improving the control performance of multi-area delayed IPS. In [19], a known finite delay is used to design H_∞ two-term frequency controller for enhancing the control performance of a two-area IPS considering communication delays, while tolerable delay margin of IPS is enhanced using time-delay in a robust H_∞ frequency controller design in [21]. The time-delay used purposefully in controller design is termed as artificial delay. Besides the above discussed control approaches, sliding mode control (SMC) approach is very effective to solve the LFC problem by designing robust state feedback controller for time-delayed multi-area IPS. SMC approach is popular for its insensitivity to parameters variation, excellent control performance and finite-time convergence [6, 30]. In [31], a non-linear sliding mode controller is designed for load frequency regulation of multi-area power system with time-varying delay. SMC scheme for LFC is considered for wind-integrated delayed IPS in [32], and SMC scheme is proposed to design a robust state feedback controller for LFC of multi-area power system with time-delay in [6, 33]. In [34], a decentralised robust load frequency controller is proposed for interconnected time-delay power system using sliding mode technique, while in [35], an event-triggered SMC design is proposed for LFC of power systems with sensor faults and communication delay. In [36], an adaptive delay-dependent sliding mode fault-tolerant LFC design is proposed for nonlinear power system with unknown time-varying state and input delays, whereas a dynamic integral SMC based LFC scheme is proposed for an interconnected delayed power system in [37].

Based on the above study, it is clearly observed that H_∞ control and SMC approaches are mostly used for the LFC design of IPS with time-delay and parametric uncertainty. The reason behind for the application of SMC approach on LFC design of delayed IPS is that SMC based controllers are very insensitive to parametric variation [37]. Similarly, the popularity of H_∞ control is widespread for its disturbance rejection performance and robustness against uncertainties [2, 19]. As time-delay and parametric uncertainty are two inevitable phenomena in LFC of IPS and they have negative impact on system stability, the effects of these phenomena on LFC should be accounted properly during LFC design for IPS. To neutralize the destabilizing effect of the existence of time-delay in a system, purposeful use of a known finite time-delay may be considered while designing the control method [38]. In view of the above discussions, to obtain the benefit of both SMC and H_∞ control methods, sliding mode controller design based on delay-dependent H_∞ stabilization criterion is proposed for load frequency regulation of IPS considering the existence of time-delay and parametric uncertainty in this paper. The main contributions of this paper are described as follows:

- Two new SMC laws are proposed considering two different controller structures, including state feedback controller and delayed feedback controller designing strategies, for load frequency regulation of delayed IPS with parametric uncertainty. Chattering is a major issue in SMC approach because it degrades control performance [33]. This paper takes care of the chattering issue of SMC approach to ensure that the controller output signals are free from chattering.
- A novel sliding surface with the incorporation of artificial delay is defined to obtain the proposed SMC law based on delayed feedback controller designing strategy. An important feature of the proposed SMC law based on delayed feedback controller designing strategy is that a finite known delay is introduced judiciously in the proposed sliding mode LFC structure to improve closed-loop IPS performance which is degraded due to the existence of time-delay in uncontrolled IPS.
- New delay-dependent H_∞ stabilization criteria in LMI framework for the sliding mode dynamics of IPS are derived by using a simple Lyapunov–Krasovskii (LK) functional approach. These stabilization criteria satisfy parametric uncertainty and time-delay existence of the closed-loop IPS, while the gains of the proposed sliding mode controllers are computed by solving these stabilization criteria. The inclusion of H_∞ criterion into the stabilization condition improves disturbance rejection performance.
- A well-known numerical example of a two-area IPS with time-delay and parametric uncertainty is considered to study the performance of the proposed load frequency regulation method. The performance of the proposed frequency regulation method is compared with some existing methods [19, 21] to show its superiority.

Notation: Throughout this paper, the superscript 'T' stands for matrix transposition, the superscript '-1' stands for matrix inverse. For any arbitrary matrix B and two symmetric matrices A and C, $\begin{bmatrix} A & B \\ * & C \end{bmatrix}$ denotes a symmetric matrix, where $*$ represents B^T.

2 Modeling of delayed interconnected power system (IPS)

A two-area IPS with time-delay in each control area is considered in this paper to analyse the LFC problem. The LFC model of the two-area IPS with time-delay in each control area is presented in Fig. 1 [19].

From Fig. 1, the dynamic model of the two-area IPS with time-delay can be described as [21]:

$$\Delta\dot{P}_{mi}(t) = \frac{1}{T_{chi}}(\Delta P_{vi}(t) - \Delta P_{mi}(t)), \tag{1}$$

$$\Delta\dot{E}_i(t) = k_i(\Delta P_{12}(t) + B_i\Delta f_i(t)), \tag{2}$$

$$\Delta\dot{P}_{12}(t) = 2\pi T_1(\Delta f_1(t) - \Delta f_2(t)), \tag{3}$$

$$\Delta\dot{P}_{vi}(t) = -\frac{1}{T_{gi}}(\frac{\Delta f_i(t)}{R_i} + \Delta P_{vi}(t) + \Delta E_i(t-\tau_i) - u_i(t)), \tag{4}$$

$$\Delta\dot{f}_i(t) = -\frac{k_{pi}}{T_{pi}}\left(\Delta P_{di}(t) + \Delta P_{ij}(t) - \Delta P_{mi}(t)\right) - \frac{\Delta f_i(t)}{T_{pi}}, \tag{5}$$

with $\Delta P_{12} = -\Delta P_{21}, i, j = 1, 2,\ i \neq j.$

The above dynamic model can be represented in state-space form as [2]:

$$\dot{x}(t) = Ax(t) + A_{d1}x(t-\tau_1) + A_{d2}x(t-\tau_2) + Bu(t) + Dw(t), \tag{6}$$

$$y(t) = Cx(t), \tag{7}$$

where the state vector

$$\begin{aligned} x(t) &= \left[\Delta Ae1(t)\ \ \Delta P_{12}(t)\ \ \Delta Ae2(t)\right]^T, \\ \Delta Ae1(t) &= \left[\Delta f_1(t)\ \ \Delta P_{m1}(t)\ \ \Delta P_{v1}(t)\ \ \Delta E_1(t)\right], \\ \Delta Ae2(t) &= \left[\Delta f_2(t)\ \ \Delta P_{m2}(t)\ \ \Delta P_{v2}(t)\ \ \Delta E_2(t)\right], \end{aligned}$$

and load disturbance vector
$w(t) = \left[\Delta P_{d1}(t)\ \ \Delta P_{d2}(t)\right]^T$.

Here, $\Delta P_{d1}(t)$ and $\Delta P_{d2}(t)$ are norm bounded, and satisfy $\|\Delta P_{d1}(t)\| < b_1$ and $\|\Delta P_{d2}(t)\| < b_2$. b_1 and b_2 are positive constants, while τ_1 and τ_2 are time delays of area 1 and area 2, respectively. The system parameters are given for $e = 1, 2$ as:

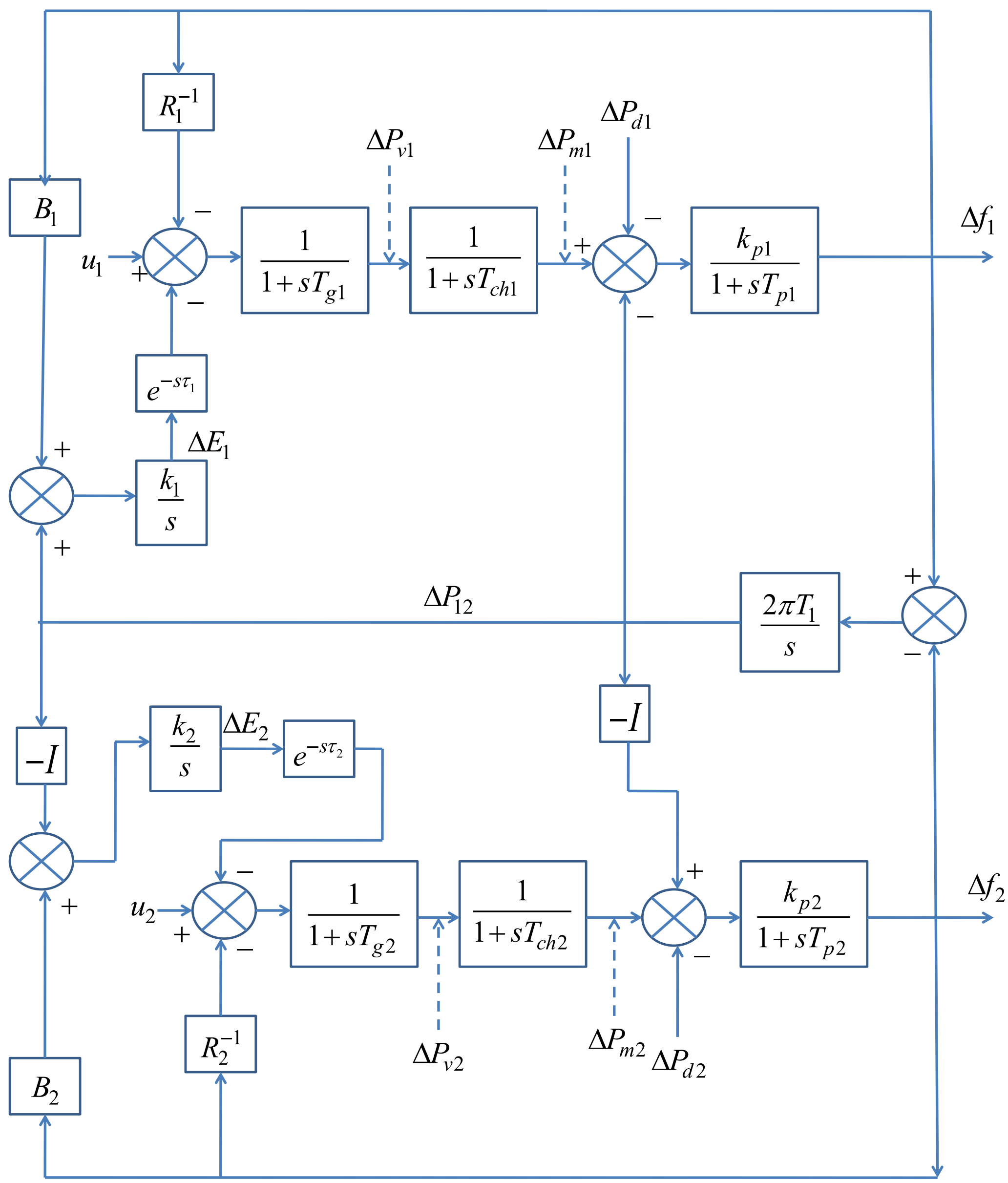

Fig. 1 LFC model of two-area IPS with time-delay

$$A = \begin{bmatrix} A_1 & A_3 & 0_{4\times4} \\ A_5 & 0_{1\times1} & -A_5 \\ 0_{4\times4} & A_4 & A_2 \end{bmatrix},\ A_e = \begin{bmatrix} -\frac{1}{T_{pe}} & \frac{k_{pe}}{T_{pe}} & 0 & 0 \\ 0 & -\frac{1}{T_{che}} & \frac{1}{T_{che}} & 0 \\ -\frac{1}{R_e T_{ge}} & 0 & -\frac{1}{T_{ge}} & 0 \\ k_e B_e & 0 & 0 & 0 \end{bmatrix},$$

$$A_3 = \begin{bmatrix} -\frac{k_{p1}}{T_{p1}} & 0 & 0 & k_1 \end{bmatrix}^T,\ A_4 = \begin{bmatrix} -\frac{k_{p2}}{T_{p2}} & 0 & 0 & k_2 \end{bmatrix}^T,\ A_5 = \begin{bmatrix} 2\pi T_{12} & 0 & 0 & 0 \end{bmatrix},$$

$$A_{d1} = \begin{bmatrix} 0_{2\times3} & 0_{2\times1} & 0_{2\times5} \\ 0_{1\times3} & -\frac{1}{T_{g1}} & 0_{1\times5} \\ 0_{6\times3} & 0_{6\times1} & 0_{6\times5} \end{bmatrix},\ A_{d2} = \begin{bmatrix} 0_{7\times8} & 0_{7\times1} \\ 0_{1\times8} & -\frac{1}{T_{g2}} \\ 0_{1\times8} & 0_{1\times1} \end{bmatrix},$$

$$B = \begin{bmatrix} 0 & 0 & -\frac{1}{T_{g1}} & 0 & 0 & 0 & 0 & 0 & 0 \\ 0 & 0 & 0 & & 0 & 0 & 0 & 0 & \frac{1}{T_{g2}} & 0 \end{bmatrix}^T,$$

$$C = \begin{bmatrix} 1 & 0 & 0 & 0 & 0 & 0 & 0 & 0 & 0 & 0 \\ 0 & 0 & 0 & 0 & 0 & 1 & 0 & 0 & 0 & 0 \end{bmatrix},\ D = \begin{bmatrix} \frac{k_{p1}}{T_{p1}} & 0 & 0 & 0 & 0 & 0 & & 0 & 0 & 0 \\ 0 & & 0 & 0 & 0 & 0 & \frac{k_{p2}}{T_{p2}} & 0 & 0 & 0 \end{bmatrix}^T.$$

Considering parametric uncertainties in system matrices of (6), one may write:

$$\begin{aligned} \dot{x}(t) &= \hat{A}(t)x(t) + \hat{A}_{d1}(t)x(t-\tau_1) \\ &\quad + \hat{A}_{d2}(t)x(t-\tau_2) + Bu(t) + Dw(t), \end{aligned} \tag{8}$$

where $\hat{A}(t)$, $\hat{A}_{d1}(t)$ and $\hat{A}_{d2}(t)$ are uncertain state matrices, i.e., $\hat{A}(t) = A + \Delta A(t)$, $\hat{A}_{d1}(t) = A_{d1} + \Delta A_{d1}(t)$ and $\hat{A}_{d2}(t) = A_{d2} + \Delta A_{d2}(t)$. $\Delta A(t)$, $\Delta A_{d1}(t)$ and $\Delta A_{d2}(t)$ are uncertainties with the system matrices A, A_{d1} and A_{d2}, respectively. The uncertainty in system matrices can be considered to be bounded with norm, and can be described as:

$$\begin{bmatrix} \Delta A(t) & \Delta A_{d1}(t) & \Delta A_{d2}(t) \end{bmatrix} = \begin{bmatrix} HF(t)E_1 & HF(t)E_2 & HF(t)E_3 \end{bmatrix}, \tag{9}$$

where H, E_1, E_2, and E_3 are constant matrices with appropriate dimensions. $F(t)$ is a time-varying matrix, which satisfies $F^T(t)F(t) \leq I$.

3 Controller designing strategy

This paper aims to design load frequency controllers based on sliding mode control for delayed IPS, whereas they satisfy the H_∞ criterion, defined as [2]:

$$\|T_{wy}\|_\infty = \frac{\|y\|_2}{\|w\|_2} = \frac{\sqrt{\int_0^\infty y^T(t)y(t)dt}}{\sqrt{\int_0^\infty w^T(t)w(t)dt}} \leq \gamma, \tag{10}$$

where γ is the H_∞ performance indicator, which indicates rejection of load disturbance. Minimization of γ is required to obtain the minimal effect of load variation in the IPS performance.

The controller designing strategy proposed for load frequency regulation of the two-area IPS with time-delay is shown in Fig. 2. As shown, state vector ($x(t)$) of the two-area delayed IPS acts as input to the proposed sliding mode controller, and the controller outputs (u_1 and u_2) act as control inputs to the two-area delayed IPS, provided that the controller gains are based on H_∞ performance condition (10). Some steps are required to compute H_∞ performance-based gains of the sliding mode controller, which are described as follows.

- *Step-1* Selection of switching surface, which is a function of the state vector of delayed IPS.
- *Step-2* Differentiate the selected switching surface and obtain an equivalent controller by equating this differentiation to zero.
- *Step-3* Obtain the closed-loop sliding mode dynamics of delayed IPS by using the equivalent controller in the state-space form of delayed IPS.
- *Step-4* Develop delay-dependent H_∞ stabilization criterion in LMI framework for the closed-loop sliding mode dynamics of delayed IPS.
- *Step-5* Obtain H_∞ performance-based gains of sliding mode controller from the solution of delay-dependent H_∞ stabilization criterion.

After obtaining the H_∞ performance-based controller gains, sliding mode control law is designed by using these

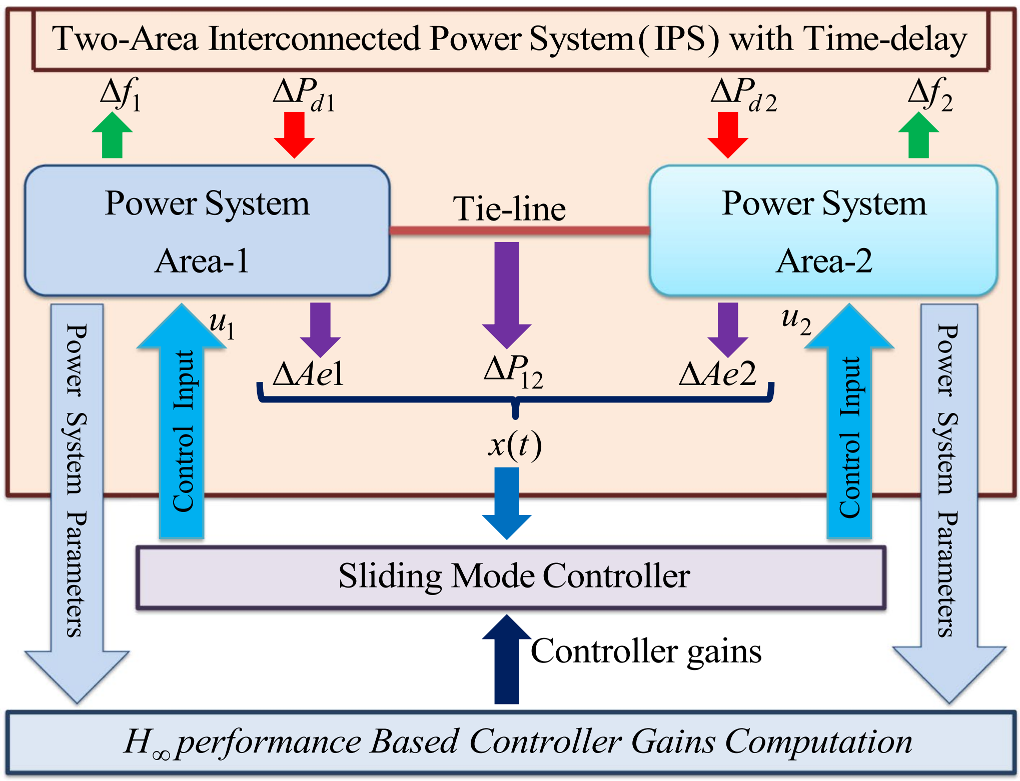

Fig. 2 Controller designing strategy for load frequency regulation of two-area IPS with time-delay

gains and system state vector for load frequency regulation of IPS with time-delay.

Subsequently, it proceeds to design the proposed H_∞ performance-based sliding mode controller by using both state feedback controller designing strategy and delayed feedback controller designing strategy.

3.1 Robust H_∞ state feedback sliding mode controller designing strategy

3.1.1 *Selection of switching surface*

A switching surface can be selected considering delay in IPS as [6]:

$$\sigma(t) = Jx(t) - \int_0^t J\hat{A}(t)x(\tau)d\tau + \int_0^t JBKx(\tau)d\tau - \int_0^{t-\tau_1} J\hat{A}_{d1}(t)x(\tau)d\tau - \int_0^{t-\tau_2} J\hat{A}_{d2}(t)x(\tau)d\tau, \quad (11)$$

where J and K are two constant matrices, and J is selected such that the matrix JB becomes nonsingular. Time derivative of (11) is given as:

$$\dot{\sigma}(t) = J\dot{x}(t) - J\hat{A}(t)x(t) + JBKx(t) - J\hat{A}_{d1}(t)x(t-\tau_1) - J\hat{A}_{d2}(t)x(t-\tau_2). \quad (12)$$

When delayed IPS trajectory reaches its sliding mode, the conditions of $\sigma(t) = 0$ and $\dot{\sigma}(t) = 0$ are satisfied by the switching function. Substituting (8) in (12), one can obtain:

$$\dot{\sigma}(t) = JBKx(t) + JBu(t) + JDw(t). \quad (13)$$

The following equivalent controller can be obtained from (13) by considering $\dot{\sigma}(t) = 0$:

$$u(t)_{equ} = -Kx(t) - (JB)^{-1}JDw(t). \quad (14)$$

The closed-loop system of delayed IPS is obtained by substituting (14) in (8) as:

$$\dot{x}(t) = \hat{A}(t)x(t) + \hat{A}_{d1}(t)x(t-\tau_1) + \hat{A}_{d2}(t)x(t-\tau_2) - BKx(t) + \hat{D}w(t), \quad (15)$$

where matrix $\hat{D} = D - B(JB)^{-1}JD$. System (15) without parametric uncertainty can be written as:

$$\dot{x}(t) = Ax(t) + A_{d1}x(t-\tau_1) + A_{d2}x(t-\tau_2) - BKx(t) + \hat{D}w(t). \quad (16)$$

Remark 1 The equivalent controller structure (14) contains an inverse matrix of $(JB)^{-1}$. It is well known that a singular matrix can not be inverted, and thus, matrix JB must be a nonsingular matrix. Therefore, care must be taken while selecting matrix J for the construction of the switching surface (11).

3.1.2 Robust H_∞ stabilization criterion

Theorem 1 *Closed-loop IPS (15) satisfies the H_∞ criterion $\|T_{wy}\| \le \gamma$ and $\gamma > 0$, if there exist positive definite matrices $\hat{P}$, $\hat{Q}_1$, $\hat{Q}_2$, $\hat{R}_{\tau_1}$, $\hat{R}_{\tau_2}$ and matrix G, such that an LMI holds as follows:*

$$\begin{bmatrix} \bar{\Lambda} & \bar{\Gamma}_1 & \bar{\Gamma}_2 & \bar{\Gamma}_3 & \bar{\Gamma}_4 & \bar{\Gamma}_5 \\ * & -\varepsilon_1 I & 0 & 0 & 0 & 0 \\ * & * & -\varepsilon_2 I & 0 & 0 & 0 \\ * & * & * & -\varepsilon_3 I & 0 & 0 \\ * & * & * & * & -\gamma^2 & 0 \\ * & * & * & * & * & -I \end{bmatrix} < 0, \tag{17}$$

where

$$\bar{\Lambda} = \begin{bmatrix} \bar{\Lambda}_{11} & \bar{\Lambda}_{12} & \bar{\Lambda}_{13} & \bar{\Lambda}_{14} \\ * & \bar{\Lambda}_{22} & \bar{\Lambda}_{23} & \bar{\Lambda}_{24} \\ * & * & \bar{\Lambda}_{33} & \bar{\Lambda}_{34} \\ * & * & * & \bar{\Lambda}_{44} \end{bmatrix},$$

and n is the dimension of $x(t)$.

$$\begin{aligned}
\bar{\Lambda}_{11} &= AY^T + YA^T - BG - G^TB^T + \hat{Q}_1 + \hat{Q}_2 - \hat{R}_{\tau_1} - \hat{R}_{\tau_2} + \sum_{i=1}^{3} \varepsilon_i HH^T, \\
\bar{\Lambda}_{12} &= A_{d1}Y^T + YA^T - G^TB^T + \hat{R}_{\tau_1} + \sum_{i=1}^{3} \varepsilon_i HH^T, \\
\bar{\Lambda}_{13} &= A_{d2}Y^T + YA^T - G^TB^T + \hat{R}_{\tau_2} + \sum_{i=1}^{3} \varepsilon_i HH^T, \\
\bar{\Lambda}_{14} &= -Y^T + YA^T - G^TB^T + \hat{P} + \sum_{i=1}^{3} \varepsilon_i HH^T, \\
\bar{\Lambda}_{22} &= A_{d1}Y^T + YA_{d1}^T - \hat{Q}_1 - \hat{R}_{\tau_1} + \sum_{i=1}^{3} \varepsilon_i HH^T, \\
\bar{\Lambda}_{23} &= A_{d2}Y^T + YA_{d1}^T + \sum_{i=1}^{3} \varepsilon_i HH^T, \\
\bar{\Lambda}_{24} &= -Y^T + YA_{d1}^T + \sum_{i=1}^{3} \varepsilon_i HH^T, \\
\bar{\Lambda}_{33} &= A_{d2}Y^T + YA_{d2}^T - \hat{Q}_2 - \hat{R}_{\tau_2} + \sum_{i=1}^{3} \varepsilon_i HH^T, \\
\bar{\Lambda}_{34} &= -Y^T + YA_{d2}^T + \sum_{i=1}^{3} \varepsilon_i HH^T, \\
\bar{\Lambda}_{44} &= -Y^T - Y + \tau_1^2\hat{R}_{\tau_1} + \tau_2^2\hat{R}_{\tau_2} + \sum_{i=1}^{3} \varepsilon_i HH^T, \\
\bar{\Gamma}_1 &= \begin{bmatrix} E_1Y^T & 0_{1n\times 3n} \end{bmatrix}^T, \bar{\Gamma}_2 = \begin{bmatrix} 0_{1n\times 1n} & E_2Y^T & 0_{1n\times 2n} \end{bmatrix}^T, \\
\bar{\Gamma}_3 &= \begin{bmatrix} 0_{1n\times 2n} & E_3Y^T & 0_{1n\times 1n} \end{bmatrix}^T, \bar{\Gamma}_4 = \begin{bmatrix} \hat{D}^T & \hat{D}^T & \hat{D}^T & \hat{D}^T \end{bmatrix}^T, \\
\bar{\Gamma}_5 &= \begin{bmatrix} CY^T & 0_{1n\times 3n} \end{bmatrix}^T,
\end{aligned}$$

The corresponding robust H_∞ controller gain matrix is obtained as $K = G\left(Y^T\right)^{-1}$.

Proof For investigating the stability of (15), the LK functional [39] is considered as:

$$V(t) = x^T(t)Px(t) + \sum_{k=1}^{2} V_k(t), \tag{18}$$

where

$$V_k(t) = \int_{t-\tau_k}^{t} x^T(s)Q_k x(s)ds + \tau_k \int_{t-\tau_k}^{t}\int_{s}^{t} \dot{x}^T(\phi)R_{\tau_k}\dot{x}(\phi)d\phi ds.$$

Differentiating (18) yields:

$$\begin{aligned}\dot{V}(t) =& 2x^T(t)P\dot{x}(t) + \dot{x}^T(t)\left[\sum_{k=1}^{2}\tau_k^2 R_{\tau_k}\right]\dot{x}(t)\\ &+ \sum_{k=1}^{2}\left[x^T(t)Q_k x(t) - x^T(t-\tau_k)Q_k x(t-\tau_k)\right.\\ &\left.-\tau_k \int_{t-\tau_k}^{t} \dot{x}^T(s)R_{\tau_k}\dot{x}(s)ds\right].\end{aligned} \tag{19}$$

Referring to Lemma 1 of [40], the integral terms in (19) may be replaced with inequalities as:

$$\begin{aligned}\dot{V}(t) \leq& 2x^T(t)P\dot{x}(t) + \dot{x}^T(t)\left[\sum_{k=1}^{2}\tau_k^2 R_{\tau_k}\right]\dot{x}(t)\\ &+ \sum_{k=1}^{2}\left[x^T(t)Q_k x(t) - x^T(t-\tau_k)Q_k x(t-\tau_k)\right.\\ &\left.+\begin{bmatrix} x(t)\\ x(t-\tau_k)\end{bmatrix}^T \begin{bmatrix} -R_{\tau_k} & R_{\tau_k}\\ * & -R_{\tau_k}\end{bmatrix}\begin{bmatrix} x(t)\\ x(t-\tau_k)\end{bmatrix}\right].\end{aligned} \tag{20}$$

Stabilization condition requires information regarding system dynamics. Therefore, the zero-valued quadratic formulation of IPS dynamics (15) is considered to incorporate IPS dynamics in the stabilization criterion instead of replacing $\dot{x}(t)$ in (20) directly by using (15), i.e.:

$$\begin{aligned}&2\xi^T(t)S\Big[-\dot{x}(t) + \hat{A}(t)x(t) + \hat{A}_{d1}(t)x(t-\tau_1)\\ &+\hat{A}_{d2}(t)x(t-\tau_2) - BKx(t) + \hat{D}w(t)\Big] = 0,\end{aligned} \tag{21}$$

where $\xi(t) = \left[x^T(t)\ x^T(t-\tau_1)\ x^T(t-\tau_2)\ \dot{x}^T(t)\right]^T$, and $S = \left[S_1^T\ S_2^T\ S_3^T\ S_4^T\right]^T$. S_1, S_2, S_3 and S_4 are proper dimensional arbitrary matrices. The above zero term (21) is able to fulfill the requirement of involving system states in stability condition. One can rewrite (21) by splitting certain and uncertain terms as:

$$\begin{aligned}&2\xi^T(t)S\{-\dot{x}(t) + Ax(t)\\ &+A_{d1}x(t-\tau_1) + A_{d2}x(t-\tau_2)\\ &-BKx(t) + \hat{D}w(t)\Big\}\\ &+ 2\xi^T(t)S\{\Delta Ax(t) + \Delta A_{d1}x(t-\tau_1)\\ &+\Delta A_{d2}x(t-\tau_2)\} = 0.\end{aligned} \tag{22}$$

The certain terms in (22) can be written as:

$$\begin{aligned}&2\xi^T(t)S\{-\dot{x}(t) + Ax(t) + A_{d1}x(t-\tau_1) + A_{d2}x(t-\tau_2)\\ &-BKx(t) + \hat{D}w(t)\Big\} = \xi^T(t)\bar{\Theta}\xi(t) + 2\xi^T(t)\bar{\theta}w(t),\end{aligned} \tag{23}$$

where $\bar{\Theta} = \left[\bar{\Theta}_{lm}\right]_{l,m=1,2,3,4}$,

$$\begin{aligned}\bar{\Theta}_{11} =& S_1A + A^TS_1^T - S_1BK - K^TB^TS_1^T,\\ \bar{\Theta}_{12} =& S_1A_{d1} + A^TS_2^T - K^TB^TS_2^T,\\ \bar{\Theta}_{13} =& S_1A_{d2} + A^TS_3^T - K^TB^TS_3^T,\\ \bar{\Theta}_{14} =& -S_1 + A^TS_4^T - K^TB^TS_4^T,\\ \bar{\Theta}_{22} =& S_2A_{d1} + A_{d1}^TS_2^T, \bar{\Theta}_{23} = S_2A_{d2} + A_{d1}^TS_3^T,\\ \bar{\Theta}_{24} =& -S_2 + A_{d1}^TS_4^T, \bar{\Theta}_{33} = S_3A_{d2} + A_{d2}^TS_3^T,\\ \bar{\Theta}_{34} =& -S_3 + A_{d2}^TS_4^T, \bar{\Theta}_{44} = -S_4 - S_4^T,\\ \bar{\theta} =& \left[\hat{D}^TS_1^T\ \hat{D}^TS_2^T\ \hat{D}^TS_3^T\ \hat{D}^TS_4^T\right]^T.\end{aligned}$$

The second term in the right hand side (RHS) of (23) can be expressed as [41]:

$$2\xi^T(t)\bar{\theta}w(t) \le \gamma^{-2}\xi^T(t)\bar{\theta}\bar{\theta}^T\xi(t) + \gamma^2 w^T(t)w(t). \tag{24}$$

Substituting (24) into (23) yields:

$$\begin{aligned}&2\xi^T(t)S\{-\dot{x}(t) + Ax(t) + A_{d1}x(t-\tau_1)\\&+A_{d2}x(t-\tau_2) - BKx(t) + \hat{D}w(t)\Big\}\\&\le \xi^T(t)\bar{\Theta}\xi(t) + \gamma^{-2}\xi^T(t)\bar{\theta}\bar{\theta}^T\xi(t) + \gamma^2 w^T(t)w(t).\end{aligned} \tag{25}$$

By following Lemma 2 of [40], the uncertain terms of (22) may be represented as:

$$\begin{aligned}&2\xi^T(t)S\{(HF(t)E_1)x(t)\\&+(HF(t)E_2)x(t-\tau_1) + (HF(t)E_3)x(t-\tau_2)\}\\&\le \sum_{j=1}^{3}\varepsilon_j\xi^T(t)\bar{\varphi}\xi(t) + \xi^T(t)\sum_{j=1}^{3}\Xi_j\xi(t),\end{aligned} \tag{26}$$

where

$$\bar{\varphi} = SHH^TS^T, \Xi_1 = \begin{bmatrix}\varepsilon_1^{-1}E_1^TE_1 & 0_{1n\times3n}\\ 0_{3n\times1n} & 0_{3n\times3n}\end{bmatrix},$$

$$\Xi_2 = \begin{bmatrix}0_{1n\times1n} & 0_{1n\times1n} & 0_{1n\times2n}\\ 0_{1n\times1n} & \varepsilon_2^{-1}E_2^TE_2 & 0_{1n\times2n}\\ 0_{2n\times1n} & 0_{2n\times1n} & 0_{2n\times2n}\end{bmatrix}, \Xi_3 = \begin{bmatrix}0_{2n\times2n} & 0_{2n\times1n} & 0_{2n\times1n}\\ 0_{1n\times2n} & \varepsilon_3^{-1}E_3^TE_3 & 0_{1n\times1n}\\ 0_{1n\times2n} & 0_{1n\times1n} & 0_{1n\times1n}\end{bmatrix}.$$

Substituting (25) and (26) into (22) yields:

$$\begin{aligned}&\xi^T(t)\bar{\Theta}\xi(t) + \gamma^{-2}\xi^T(t)\bar{\theta}\bar{\theta}^T\xi(t) + \gamma^2 w^T(t)w(t)\\&\quad + \sum_{j=1}^{3}\varepsilon_j\xi^T(t)\bar{\varphi}\xi(t) + \xi^T(t)\sum_{j=1}^{3}\Xi_j\xi(t) \ge 0.\end{aligned} \tag{27}$$

Addition of (20) and (27) gives:

$$\dot{V}(t) \le \xi^T(t)\left\{\bar{\Psi} + \sum_{j=1}^{3}\Xi_j + \gamma^{-2}\bar{\theta}\bar{\theta}^T\right\}\xi(t) + \gamma^2 w^T(t)w(t), \tag{28}$$

where $\bar{\Psi} = \left[\bar{\Psi}_{lm}\right]_{l,m=1,2,3,4}$,

$$\bar{\Psi}_{11} = \bar{\Theta}_{11} + Q_1 + Q_2 - R_{\tau_1} - R_{\tau_2} + \sum_{j=1}^{3}\varepsilon_j S_1HH^TS_1^T,$$

$$\bar{\Psi}_{12} = \bar{\Theta}_{12} + R_{\tau_1} + \sum_{j=1}^{3}\varepsilon_j S_1HH^TS_2^T,$$

$$\bar{\Psi}_{13} = \bar{\Theta}_{13} + R_{\tau_2} + \sum_{j=1}^{3}\varepsilon_j S_1HH^TS_3^T,$$

$$\bar{\Psi}_{14} = \bar{\Theta}_{14} + P + \sum_{j=1}^{3}\varepsilon_j S_1HH^TS_4^T,$$

$$\bar{\Psi}_{22} = \bar{\Theta}_{22} - Q_1 - R_{\tau_1} + \sum_{j=1}^{3}\varepsilon_j S_2HH^TS_2^T,$$

$$\bar{\Psi}_{23} = \bar{\Theta}_{23} + \sum_{j=1}^{3}\varepsilon_j S_2HH^TS_3^T,$$

$$\bar{\Psi}_{24} = \bar{\Theta}_{24} + \sum_{j=1}^{3}\varepsilon_j S_2HH^TS_4^T,$$

$$\bar{\Psi}_{33} = \bar{\Theta}_{33} - Q_2 - R_{\tau_2} + \sum_{j=1}^{3}\varepsilon_j S_3HH^TS_3^T,$$

$$\bar{\Psi}_{34} = \bar{\Theta}_{34} + \sum_{j=1}^{3}\varepsilon_j S_3HH^TS_4^T,$$

$$\bar{\Psi}_{44} = \bar{\Theta}_{44} + \tau_1^2R_{\tau_1} + \tau_2^2R_{\tau_2} + \sum_{j=1}^{3}\varepsilon_j S_4HH^TS_4^T.$$

A cost function is obtained from (10) for the investigation of H_∞ criterion, as:

$$J_{yw} = \int_0^\infty \left[y^T(t)y(t) - \gamma^2 w^T(t)w(t)\right]dt. \tag{29}$$

Closed-loop IPS (15) satisfies the criterion (10) only when $J_{yw} \le 0$. For initial condition $V(0) = 0$ and since $V(\infty) \ge 0$, one can write:

$$J_{yw} \le \int_0^\infty \left[y^T(t)y(t) - \gamma^2 w^T(t)w(t) + \dot{V}(t) \right] dt \quad (30)$$

Substituting (28) into (30), one obtains:

$$J_{yw} \le \int_0^\infty \xi^T(t)\bar{\Omega}\xi(t)dt, \quad (31)$$

where $\bar{\Omega} = \bar{\Psi} + \sum_{j=1}^{3} \Xi_j + \gamma^{-2}\bar{\theta}\bar{\theta}^T + \hat{C}\hat{C}^T$ and $\hat{C} = \begin{bmatrix} C & 0 & 0 & 0 \end{bmatrix}^T$.

The condition $J_{yw} \le 0$ is satisfied, if there is:

$$\bar{\Omega} < 0 \quad (32)$$

Now, using Schur complement [41] in inequality (32), we can write:

$$\begin{bmatrix} \bar{\Psi} & \bar{\Phi}_1 & \bar{\Phi}_2 & \bar{\Phi}_3 & \bar{\Phi}_4 & \bar{\Phi}_5 \\ * & -\varepsilon_1 I & 0 & 0 & 0 & 0 \\ * & * & -\varepsilon_2 I & 0 & 0 & 0 \\ * & * & * & -\varepsilon_3 I & 0 & 0 \\ * & * & * & * & -\gamma^2 I & 0 \\ * & * & * & * & * & -I \end{bmatrix} < 0, \quad (33)$$

where $\bar{\Phi}_1 = \begin{bmatrix} E_1 & 0_{1n\times 3n} \end{bmatrix}^T$, $\bar{\Phi}_2 = \begin{bmatrix} 0_{1n\times 1n} & E_2 & 0_{1n\times 2n} \end{bmatrix}^T$, $\bar{\Phi}_3 = \begin{bmatrix} 0_{1n\times 2n} & E_3 & 0_{1n\times 1n} \end{bmatrix}^T$, $\bar{\Phi}_4 = \begin{bmatrix} \hat{D}^T S_1^T & \hat{D}^T S_2^T & \hat{D}^T S_3^T & \hat{D}^T S_4^T \end{bmatrix}^T$, $\bar{\Phi}_5 = \begin{bmatrix} C & 0_{1n\times 3n} \end{bmatrix}^T$.

Considering $S_1 = S_2 = S_3 = S_4 = S$, pre- and post-multiplying with $diag\{S^{-1}\ S^{-1}\ S^{-1}\ S^{-1}\ I\ I\ I\ I\ I\}$ and its transpose in (33), and finally adopting variables change as $S^{-1} = Y$, $K(S^{-1})^T = KY^T = G$, $S^{-1}Q_1(S^{-1})^T = \hat{Q}_1$, $S^{-1}Q_2(S^{-1})^T = \hat{Q}_2$, $S^{-1}R_{\tau_1}(S^{-1})^T = \hat{R}_{\tau_1}$, $S^{-1}R_{\tau_2}(S^{-1})^T = \hat{R}_{\tau_2}$,

$S^{-1}P(S^{-1})^T = \hat{P}$, one obtains (17). Hence, proof of Theorem 1 is completed. □

Remark 2 For a specific value of γ, H_∞ controller gain matrix K may be obtained from the feasible solution of LMI (17). As per (10), the minimum value of γ should be utilized for computing controller gains to have minimal disturbance effect on system response. The minimum γ value can be obtained by minimizing γ^2 of LMI (17) and K can then be easily obtained from the solution of LMI (17) by using this γ value. But, this process results in high value of controller gains [19]. From Theorem 1, it is known that variables G and Y of LMI (17) are involved in the calculation of K. So, minimization of $\|G\|$ and $\|Y^{-1}\|$ can result in the values of K within limits. Based on the analysis, following LMI optimization problem is designed, and solution of this optimization problem gives minimum γ as well as stabilizing gain K.

LMI Optimization Problem 1:

Min $\gamma^2 + \bar{g} + \bar{y}$ Subject to (17), $\begin{bmatrix} \bar{g}I & G \\ * & I \end{bmatrix} > 0$ and $\begin{bmatrix} Y & I \\ * & \bar{y}I \end{bmatrix} > 0$.

where $\bar{y}$ and $\bar{g}$ denote the matrix norms $\|Y^{-1}\|$ and $\|G\|$, respectively.

Table 1 Parameters of the two-area IPS

Sl. No.	Parameter	Area 1	Area 2
1	T_{chi}	0.3s	0.17s
2	T_{gi}	0.1s	0.4s
3	R_i	0.05	0.05
4	k_i	0.5	0.5
5	T_{pi}	10	8
6	k_{pi}	1	0.67
7	B_i	41	81.5

Table 2 A comparative study on the two-area closed-loop IPS without considering parametric uncertainty

Approach	*h*	γ
H_∞ two-term control [19]	0.70s	4.0124
H_∞ delayed feedback control [21]	0.78s	3.2240
Proposed control approach	0.86s	2.6679

Remark 3 The LK functional defined in (18) has double integral terms whereas the LK functionals chosen in [6, 21] have single integral terms. Use of multiple integral terms in LK functional reduces conservatism of delay-dependent stabilization criterion. On the other hand, it increases the computational burden. To reduce computational burden as well as conservatism of stabilization criterion, LK functional defined in this paper is restricted to double integral terms.

The following corollary presents H_∞ performance based criterion for stabilization of delayed IPS (16).

Corollary 1 *Closed-loop IPS (16) satisfies H_∞ criterion $\left\|T_{wy}\right\| \le \gamma$ and $\gamma > 0$, for positive definite matrices $\hat{P}$, $\hat{Q}_1$, $\hat{Q}_2$, $\hat{R}_{\tau_1}$, $\hat{R}_{\tau_2}$ and arbitrary matrix G, such that an LMI holds as follows*:

$$\begin{bmatrix} \tilde{\Lambda} & \tilde{D} & \tilde{C} \\ * & -\gamma^2 & 0 \\ * & * & -I \end{bmatrix} < 0, \tag{34}$$

$$\text{where}\tilde{\Lambda} = \begin{bmatrix} \tilde{\Lambda}_{11} & \tilde{\Lambda}_{12} & \tilde{\Lambda}_{13} & \tilde{\Lambda}_{14} \\ * & \tilde{\Lambda}_{22} & \tilde{\Lambda}_{23} & \tilde{\Lambda}_{24} \\ * & * & \tilde{\Lambda}_{33} & \tilde{\Lambda}_{34} \\ * & * & * & \tilde{\Lambda}_{44} \end{bmatrix},$$

$$\begin{aligned}
\tilde{\Lambda}_{11} &= AY^T + YA^T - BG - G^TB^T + \hat{Q}_1 + \hat{Q}_2 - \hat{R}_{\tau_1} - \hat{R}_{\tau_2},\\
\tilde{\Lambda}_{12} &= A_{d1}Y^T + YA^T - G^TB^T + \hat{R}_{\tau_1},\\
\tilde{\Lambda}_{13} &= A_{d2}Y^T + YA^T - G^TB^T + \hat{R}_{\tau_2},\\
\tilde{\Lambda}_{14} &= -Y^T + YA^T - G^TB^T + \hat{P},\\
\tilde{\Lambda}_{22} &= A_{d1}Y^T + YA_{d1}^T - \hat{Q}_1 - \hat{R}_{\tau_1},\\
\tilde{\Lambda}_{23} &= A_{d2}Y^T + YA_{d1}^T, \tilde{\Lambda}_{24} = -Y^T + YA_{d1}^T,\\
\tilde{\Lambda}_{33} &= A_{d2}Y^T + YA_{d2}^T - \hat{Q}_2 - \hat{R}_{\tau_2}, \tilde{\Lambda}_{34} = -Y^T + YA_{d2}^T,\\
\tilde{\Lambda}_{44} &= -Y^T - Y + \tau_1^2\hat{R}_{\tau_1} + \tau_2^2\hat{R}_{\tau_2},\\
\tilde{D} &= \left[\hat{D}^T \ \hat{D}^T \ \hat{D}^T \ \hat{D}^T\right]^T, \tilde{C} = \left[CY^T \ 0_{1n\times 3n}\right]^T.
\end{aligned}$$

The corresponding H_∞ controller gain matrix is obtained as $K = G\left(Y^T\right)^{-1}$.

Proof One can prove Corollary 1 by adopting similar procedures as in proof of Theorem 1 without considering uncertainties of IPS parameters. □

3.1.3 Sliding mode control law based on state feedback control strategy

Theorem 2 *Switching control law satisfying reaching condition $\sigma_i(t)\dot{\sigma}_i(t) < 0$ is given by:*

$$u_i(t) = -K_ix(t) - b_i(J_iB_i)^{-1}\|J_iD_i\|\left(\frac{\sigma_i(t)}{\|\sigma_i(t)\| + \zeta}\right), \tag{35}$$

where ζ is a constant having positive value close to zero.

Proof
Proof of Theorem 2 is given in Appendix. □

Remark 4 Signum function of switching surface is generally used in sliding mode controller structure to drive system trajectory into the predefined sliding surface [6, 31, 32]. However, such controller has chattering issue, and therefore, use of signum function is avoided in design of sliding mode controller (35) to reduce the chattering effect.

3.2 Robust H_∞ delayed feedback sliding mode controller designing strategy

3.2.1 Selection of switching surface

The switching surface is selected by including artificial delay to improve the performance of closed-loop IPS, as:

$$\begin{aligned}
\sigma(t) =& Jx(t) - \int_0^t J\hat{A}(t)x(\tau)d\tau + \int_0^t JBKx(\tau)d\tau + \int_0^{t-h} JBK_hx(\tau)d\tau \\
& - \int_0^{t-\tau_1} J\hat{A}_{d1}(t)x(\tau)d\tau - \int_0^{t-\tau_2} J\hat{A}_{d2}(t)x(\tau)d\tau,
\end{aligned} \tag{36}$$

where K_h is a constant matrix, and h is the artificial delay chosen by the control designer. Derivative of (36) gives:

$$\begin{aligned}
\dot{\sigma}(t) =& J\dot{x}(t) - J\hat{A}(t)x(t) + JBKx(t) + JBK_hx(t-h) \\
& - J\hat{A}_{d1}(t)x(t-\tau_1) - J\hat{A}_{d2}(t)x(t-\tau_2).
\end{aligned} \tag{37}$$

Substituting (8) into (37) yields:

$$\dot{\sigma}(t) = JBKx(t) + JBK_hx(t-h) + JBu(t) + JDw(t). \tag{38}$$

Considering $\dot{\sigma}(t) = 0$, the equivalent controller is derived from (38) as:

$$u(t)_{equ} = -Kx(t) - K_hx(t-h) - (JB)^{-1}JDw(t). \tag{39}$$

The sliding mode closed-loop delayed IPS is obtained by substituting (39) into (8) as:

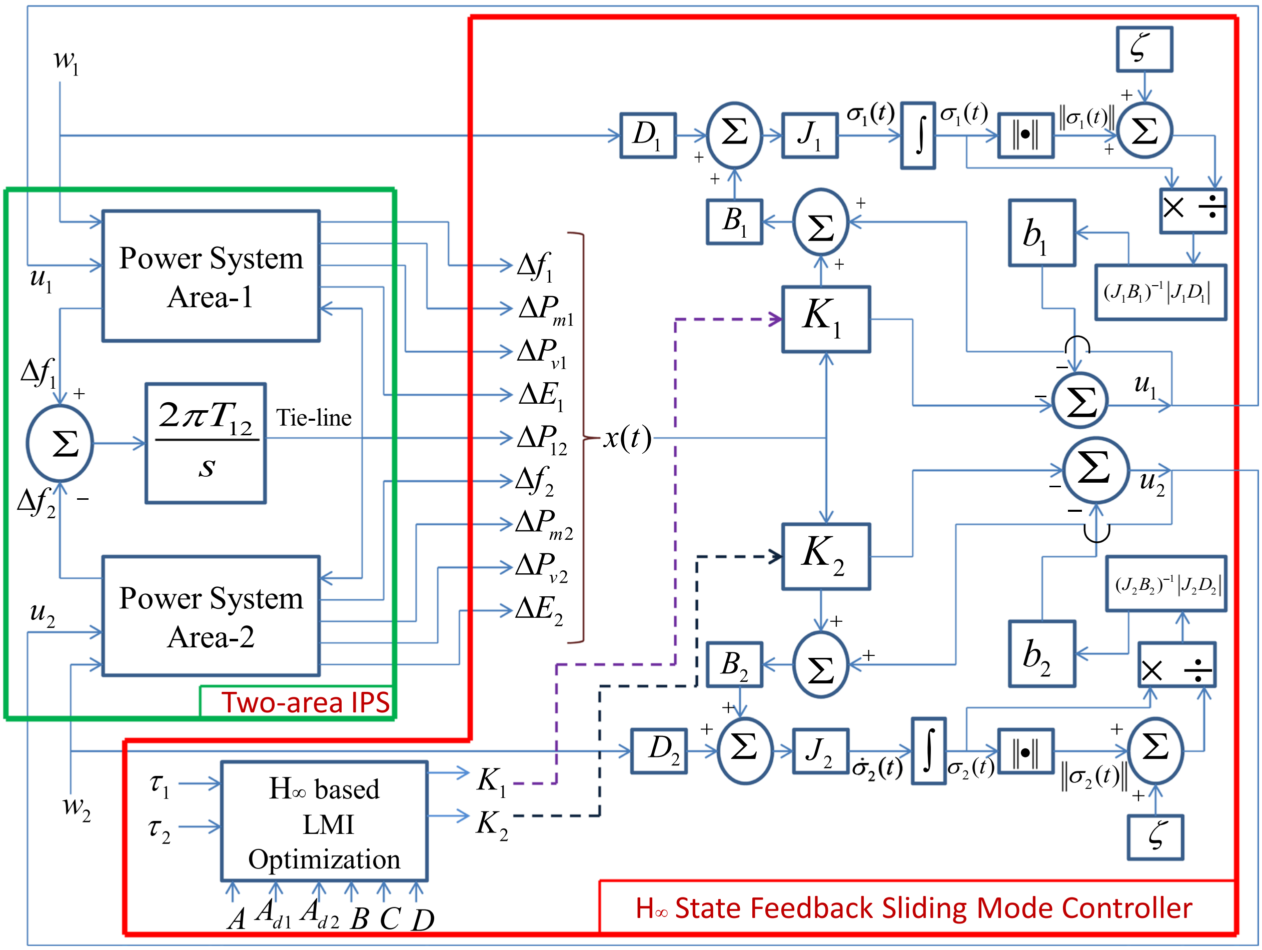

Fig. 3 H_∞ state feedback SMC model for LFC of the two-area IPS

$$\dot{x}(t) = \hat{A}(t)x(t) + \hat{A}_{d1}(t)x(t-\tau_1) + \hat{A}_{d2}(t)x(t-\tau_2) - BKx(t) - BK_hx(t-h) + \hat{D}w(t), \tag{40}$$

where matrix $\hat{D} = D - B(JB)^{-1}JD$. System (40) without parametric uncertainty can be written as:

$$\begin{aligned}\dot{x}(t) =& Ax(t) + A_{d1}x(t-\tau_1) + A_{d2}x(t-\tau_2) \\ &- BKx(t) - BK_hx(t-h) + \hat{D}w(t).\end{aligned} \tag{41}$$

3.2.2 Robust H_∞ stabilization criterion

Theorem 3 *Closed-loop IPS (40) satisfies H_∞ criterion $\|T_{wy}\| \leq \gamma$ and $\gamma > 0$, for positive definite matrices $\hat{P}$, $\hat{Q}_1$, $\hat{Q}_2$, $\hat{Q}_h$, $\hat{R}_{\tau_1}$, $\hat{R}_{\tau_2}$, $\hat{R}_h$ and arbitrary matrices G and V, such that an LMI holds as follows:*

$$\begin{bmatrix} \hat{\Omega} & \hat{\Theta}_1 & \hat{\Theta}_2 & \hat{\Theta}_3 & \hat{\Theta}_4 & \hat{\Theta}_5 \\ * & -\varepsilon_1 I & 0 & 0 & 0 & 0 \\ * & * & -\varepsilon_2 I & 0 & 0 & 0 \\ * & * & * & -\varepsilon_3 I & 0 & 0 \\ * & * & * & * & -\gamma^2 & 0 \\ * & * & * & * & * & -I \end{bmatrix} < 0, \tag{42}$$

where $\hat{\Omega} = \begin{bmatrix} \hat{\Omega}_{11} & \hat{\Omega}_{12} & \hat{\Omega}_{13} & \hat{\Omega}_{14} & \hat{\Omega}_{15} \\ * & \hat{\Omega}_{22} & \hat{\Omega}_{23} & \hat{\Omega}_{24} & \hat{\Omega}_{25} \\ * & * & \hat{\Omega}_{33} & \hat{\Omega}_{34} & \hat{\Omega}_{35} \\ * & * & * & \hat{\Omega}_{44} & \hat{\Omega}_{45} \\ * & * & * & * & \hat{\Omega}_{55} \end{bmatrix}$,

$$\hat{\Omega}_{11} = AY^T + YA^T - BG - G^TB^T + \hat{Q}_1 + \hat{Q}_2 + \hat{Q}_h - \hat{R}_h - \hat{R}_{\tau_1} - \hat{R}_{\tau_2} + \sum_{j=1}^{3} \varepsilon_j HH^T,$$

$$\hat{\Omega}_{12} = A_{d1}Y^T + YA^T - G^TB^T + \hat{R}_{\tau_1} + \sum_{j=1}^{3} \varepsilon_j HH^T,$$

$$\hat{\Omega}_{13} = A_{d2}Y^T + YA^T - G^TB^T + \hat{R}_{\tau_2} + \sum_{j=1}^{3} \varepsilon_j HH^T,$$

$$\hat{\Omega}_{14} = YA^T - BV - G^TB^T + \hat{R}_h + \sum_{j=1}^{3} \varepsilon_j HH^T,$$

$$\hat{\Omega}_{15} = -Y^T + YA^T - G^TB^T + \hat{P} + \sum_{j=1}^{3} \varepsilon_j HH^T,$$

$$\hat{\Omega}_{22} = A_{d1}Y^T + YA_{d1}^T - \hat{Q}_1 - \hat{R}_{\tau_1} + \sum_{j=1}^{3} \varepsilon_j HH^T,$$

$$\hat{\Omega}_{23} = A_{d2}Y^T + YA_{d1}^T + \sum_{j=1}^{3} \varepsilon_j HH^T,$$

$$\hat{\Omega}_{24} = -BV + YA_{d1}^T + \sum_{j=1}^{3} \varepsilon_j HH^T,$$

$$\hat{\Omega}_{25} = -Y^T + YA_{d1}^T + \sum_{j=1}^{3} \varepsilon_j HH^T,$$

$$\hat{\Omega}_{33} = A_{d2}Y^T + YA_{d2}^T - \hat{Q}_2 - \hat{R}_{\tau_2} + \sum_{j=1}^{3} \varepsilon_j HH^T,$$

$$\hat{\Omega}_{34} = -BV + YA_{d2}^T + \sum_{j=1}^{3} \varepsilon_j HH^T,$$

$$\hat{\Omega}_{35} = -Y^T + YA_{d2}^T + \sum_{j=1}^{3} \varepsilon_j HH^T,$$

$$\hat{\Omega}_{44} = -BV - V^TB^T - \hat{Q}_h - \hat{R}_h + \sum_{j=1}^{3} \varepsilon_j HH^T,$$

$$\hat{\Omega}_{45} = -Y^T - V^TB^T + \sum_{j=1}^{3} \varepsilon_j HH^T,$$

$$\hat{\Omega}_{55} = -Y^T - Y + \tau_1^2\hat{R}_{\tau_1} + \tau_2^2\hat{R}_{\tau_2} + h^2\hat{R}_h + \sum_{j=1}^{3} \varepsilon_j HH^T,$$

$$\hat{\Theta}_1 = \left[E_1 Y^T \ 0_{1n\times 4n}\right]^T, \hat{\Theta}_2 = \left[0_{1n\times 1n} \ E_2 Y^T \ 0_{1n\times 3n}\right]^T,$$
$$\hat{\Theta}_3 = \left[0_{1n\times 2n} \ E_3 Y^T \ 0_{1n\times 2n}\right]^T,$$
$$\hat{\Theta}_4 = \left[\hat{D}^T \ \hat{D}^T \ \hat{D}^T \ \hat{D}^T \ \hat{D}^T\right]^T,$$
$$\hat{\Theta}_5 = \left[C Y^T \ 0_{1n\times 4n}\right]^T$$

The corresponding robust H_∞ controller gain matrices are obtained as $K = G\left(Y^T\right)^{-1}$ and $K_h = V\left(Y^T\right)^{-1}$.

Proof To investigate the stability of (40), the LK functional is considered as:

$$V(t) = x^T(t)Px(t) + V_h(t) + \sum_{j=1}^{2} V_j(t), \quad (43)$$

where

$$V_h(t) = \int_{t-h}^{t} x^T(\theta)Q_h x(\theta)d\theta + h\int_{t-h}^{t}\int_{\theta}^{t} \dot{x}^T(\phi)R_h\dot{x}(\phi)d\phi d\theta,$$

and

$$V_j(t) = \int_{t-\tau_j}^{t} x^T(\theta)Q_j x(\theta)d\theta + \tau_1\int_{t-\tau_j}^{t}\int_{\theta}^{t} \dot{x}^T(\phi)R_{\tau_j}\dot{x}(\phi)d\phi d\theta.$$

Next, by implementing similar steps as in proof of Theorem 1, one obtains (42). This completes the proof of Theorem 3. □

LMI Optimization Problem 2:

Min $\gamma^2 + \bar{g} + \bar{\nu} + \bar{y}$

Subject to (42), $\begin{bmatrix} \bar{g}I & G \\ * & I \end{bmatrix} > 0$, $\begin{bmatrix} \bar{\nu}I & V \\ * & I \end{bmatrix} > 0$ and $\begin{bmatrix} Y & I \\ * & \bar{y}I \end{bmatrix} > 0$.

where $\bar{\nu}$ represents the norm of matrix $\|V\|$. Stabilizing gains K and K_h can be calculated by solving the above LMI optimization problem.

H_∞ performance based stabilization criterion for (41) can be deduced from Theorem 3. The following corollary presents the criterion for (41).

Corollary 2 *Closed-loop IPS (41) satisfies H_∞ criterion $\|T_{wy}\| \le \gamma$ and $\gamma > 0$, for positive definite matrices $\hat{P}$, $\hat{Q}_1$, $\hat{Q}_2$, $\hat{Q}_h$, $\hat{R}_{\tau_1}$, $\hat{R}_{\tau_2}$, $\hat{R}_h$ and arbitrary matrices G and V, such that an LMI holds as follows:*

$$\begin{bmatrix} \tilde{\varphi} & \widehat{D} & \widehat{C} \\ * & -\gamma^2 & 0 \\ * & * & -I \end{bmatrix} < 0, \quad (44)$$

where $\tilde{\varphi} = \begin{bmatrix} \tilde{\varphi}_{11} & \tilde{\varphi}_{12} & \tilde{\varphi}_{13} & \tilde{\varphi}_{14} & \tilde{\varphi}_{15} \\ * & \tilde{\varphi}_{22} & \tilde{\varphi}_{23} & \tilde{\varphi}_{24} & \tilde{\varphi}_{25} \\ * & * & \tilde{\varphi}_{33} & \tilde{\varphi}_{34} & \tilde{\varphi}_{35} \\ * & * & * & \tilde{\varphi}_{44} & \tilde{\varphi}_{45} \\ * & * & * & * & \tilde{\varphi}_{55} \end{bmatrix}$,

$$\tilde{\varphi}_{11} = AY^T + YA^T - BG - G^TB^T + \hat{Q}_1 + \hat{Q}_2 + \hat{Q}_h - \hat{R}_h - \hat{R}_{\tau_1} - \hat{R}_{\tau_2},$$
$$\tilde{\varphi}_{12} = A_{d1}Y^T + YA^T - G^TB^T + \hat{R}_{\tau_1},$$
$$\tilde{\varphi}_{13} = A_{d2}Y^T + YA^T - G^TB^T + \hat{R}_{\tau_2},$$
$$\tilde{\varphi}_{14} = YA^T - BV - G^TB^T + \hat{R}_h,$$
$$\tilde{\varphi}_{15} = -Y^T + YA^T - G^TB^T + \hat{P},$$
$$\tilde{\varphi}_{22} = A_{d1}Y^T + YA_{d1}^T - \hat{Q}_1 - \hat{R}_{\tau_1},$$
$$\tilde{\varphi}_{23} = A_{d2}Y^T + YA_{d1}^T, \tilde{\varphi}_{24} = -BV + YA_{d1}^T,$$
$$\tilde{\varphi}_{25} = -Y^T + YA_{d1}^T, \tilde{\varphi}_{33} = A_{d2}Y^T + YA_{d2}^T - \hat{Q}_2 - \hat{R}_{\tau_2},$$
$$\tilde{\varphi}_{34} = -BV + YA_{d2}^T, \tilde{\varphi}_{35} = -Y^T + YA_{d2}^T,$$
$$\tilde{\varphi}_{44} = -BV - V^TB^T - \hat{Q}_h - \hat{R}_h, \tilde{\varphi}_{45} = -Y^T - V^TB^T,$$
$$\tilde{\varphi}_{55} = -Y^T - Y + \tau_1^2\hat{R}_{\tau_1} + \tau_2^2\hat{R}_{\tau_2} + h^2\hat{R}_h,$$
$$\widehat{D} = \left[\hat{D}^T \ \hat{D}^T \ \hat{D}^T \ \hat{D}^T \ \hat{D}^T\right]^T, \widehat{C} = \left[CY^T \ 0_{1n\times 4n}\right]^T.$$

The corresponding H_∞ controller gain matrices are obtained as $K = G\left(Y^T\right)^{-1}$ and $K_h = V\left(Y^T\right)^{-1}$.

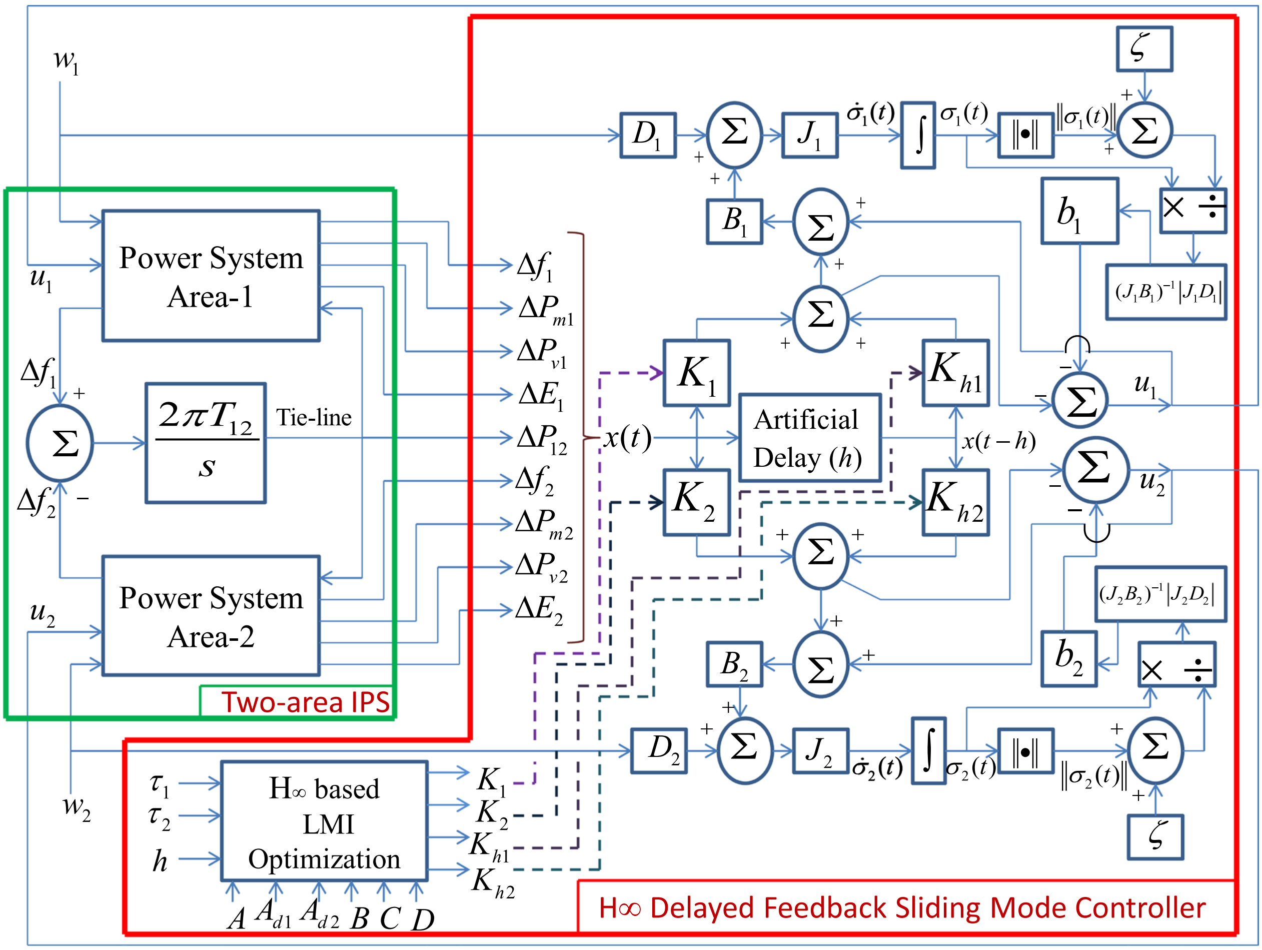

Fig. 4 H_∞ delayed feedback SMC model for LFC of the two-area IPS

Proof One may follow Theorem 3 to prove Corollary 2. □

3.2.3 Sliding mode control law based on delayed feedback control strategy

Theorem 4 *Switching control law satisfying reaching condition $\sigma_i(t)\dot{\sigma}_i(t) < 0$ is given by:*

$$u_i(t) = -K_i x(t) - K_{hi} x(t-h) - b_i (J_i B_i)^{-1} \|J_i D_i\| \left(\frac{\sigma_i(t)}{\|\sigma_i(t)\| + \zeta} \right), \tag{45}$$

Proof Proof of Theorem 4 is similar to that of Theorem 2, and thus no further description is given here. □

Remark 5 The performance of the proposed SMC scheme may be improved by selecting a suitable h value which can improve the transient stability of a delayed system. It can also be used to improve the dynamic response of a system with time-delay.

4 Results analysis

4.1 Numerical example

A well-known numerical example of an IPS with two areas is considered for analyzing the performance of the

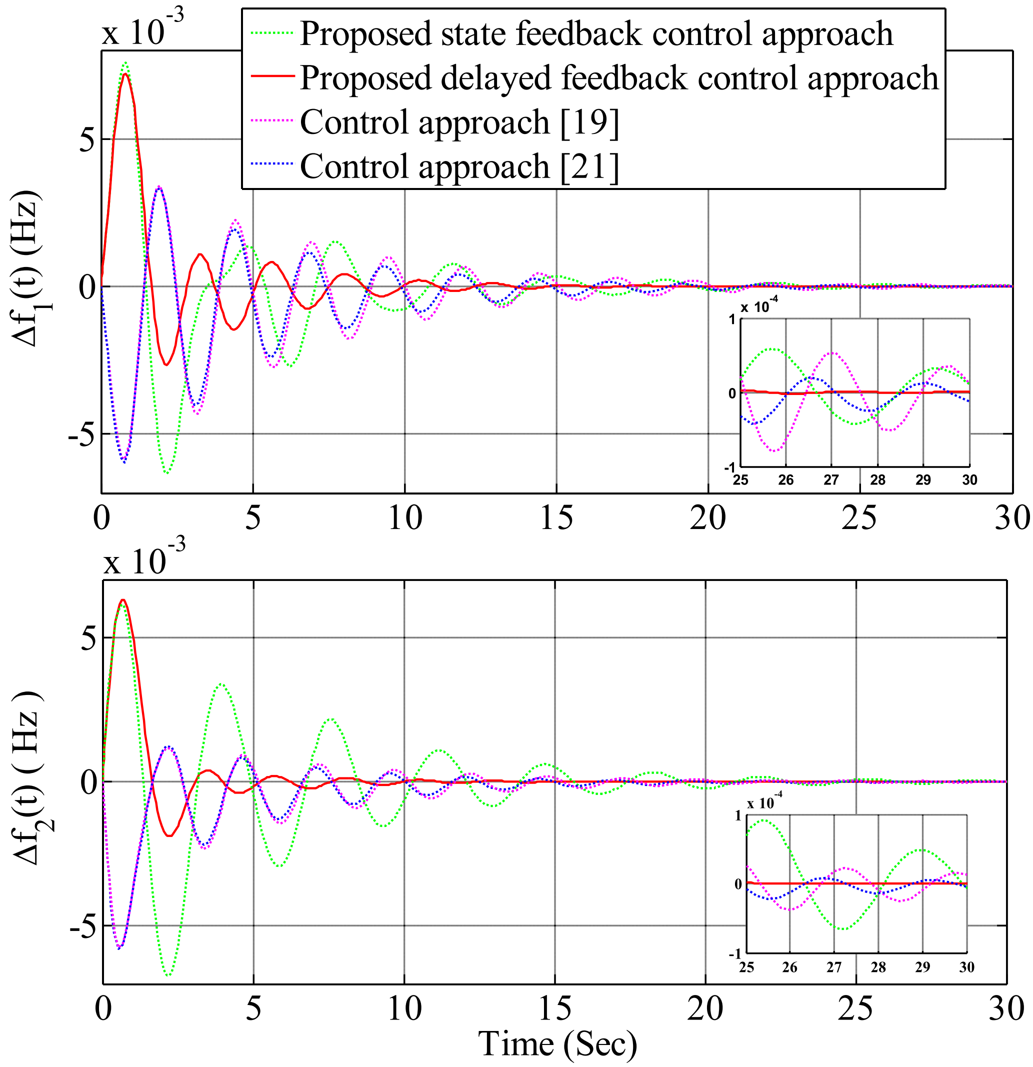

Fig. 5 Frequency deviations for step load change in the closed-loop IPS

proposed SMC schemes. Parameters of the IPS are given in Table 1 [19, 21].

The uncertainties in IPS parameters are assumed as $E_1 = E_2 = E_3 = H = 0.001I$ as described in (9). Time-delays of area-1 and area-2 are considered to be fixed as $\tau_1 = 0.1s$ and $\tau_2 = 0.2s$, respectively.

For the H_∞ state feedback sliding mode controller (35) and H_∞ delayed feedback sliding mode controller (45), the design parameters ζ and b_i are set as 0.001 and 1, respectively, whereas matrix J is selected as:

$$J = \begin{bmatrix} 10 & 0 & -0.1 & 0 & 0 & 0 & 0 & 0 & 0 \\ 0 & 0 & 0 & 0 & 0 & 12 & 0 & 0.4 & 0 \end{bmatrix}.$$

Besides ζ, b_i and J, controller gain matrix K is required to design controller (35), and an artificial delay (h) and controller gains (K and K_h) are needed to design controller (45). h is tuned at 0.86s, while LMI Optimization

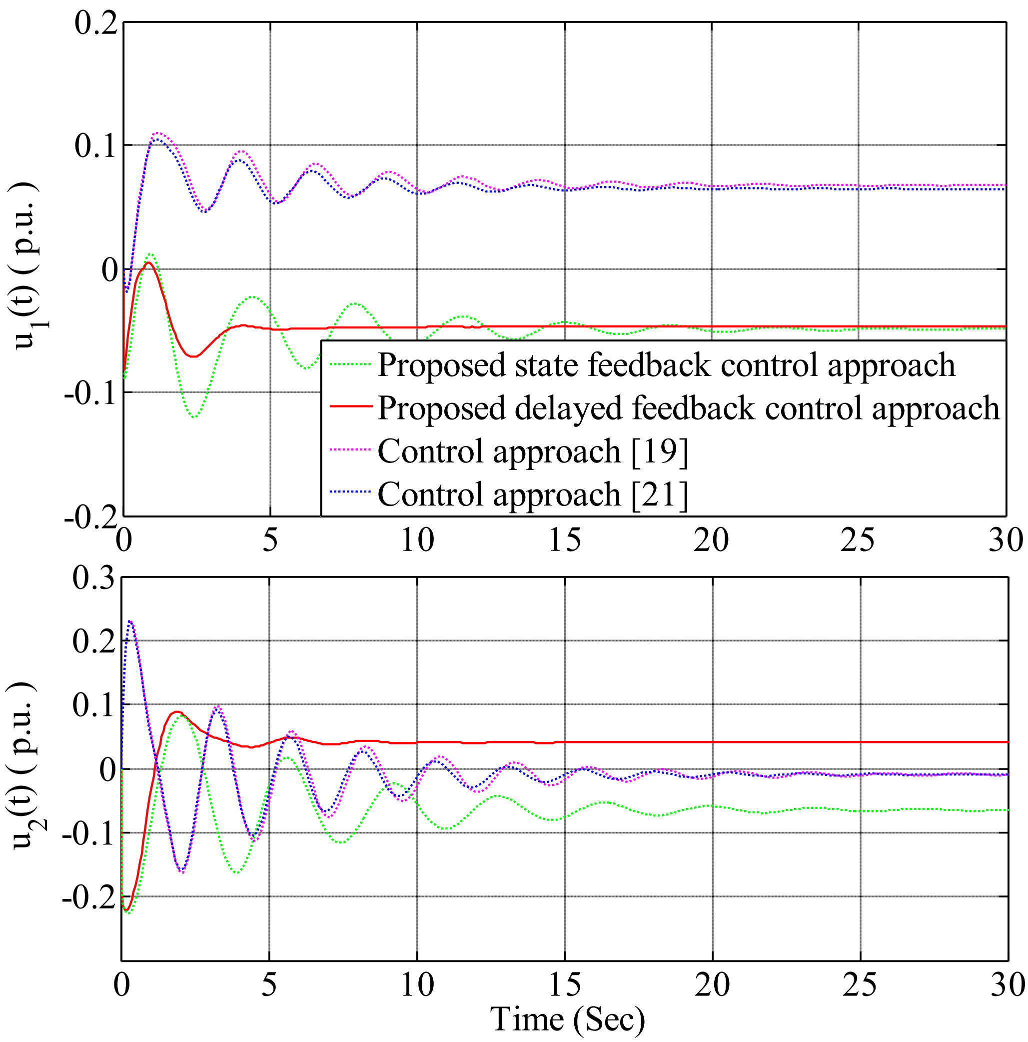

Fig. 6 Control inputs to the closed-loop IPS with step load change

Problem 1 and Problem 2 are solved by using mincx solver of LMI control Toolbox in MATLAB to obtain H_∞ performance index γ and gains of controllers (35) and (45), respectively. γ for controller (35) is computed as 1.4942 and the corresponding gain matrix K is presented in (46). Similarly, γ for controller (45) is computed as 2.6686 and the corresponding gain matrices K and K_h are presented in (47) and (48). Replacing (17) with (34) in LMI Optimization Problem 1 and (42) with (44) in LMI Optimization Problem 2, H_∞ performance index and gains of controllers (35) and (45) are computed neglecting the uncertainties of IPS parameters. At this condition, γ is obtained as 1.4938 and K is computed as (49) for controller (35). Similarly, for controller (45), γ is obtained as 2.6679, and K and K_h are computed as (50) and (51).

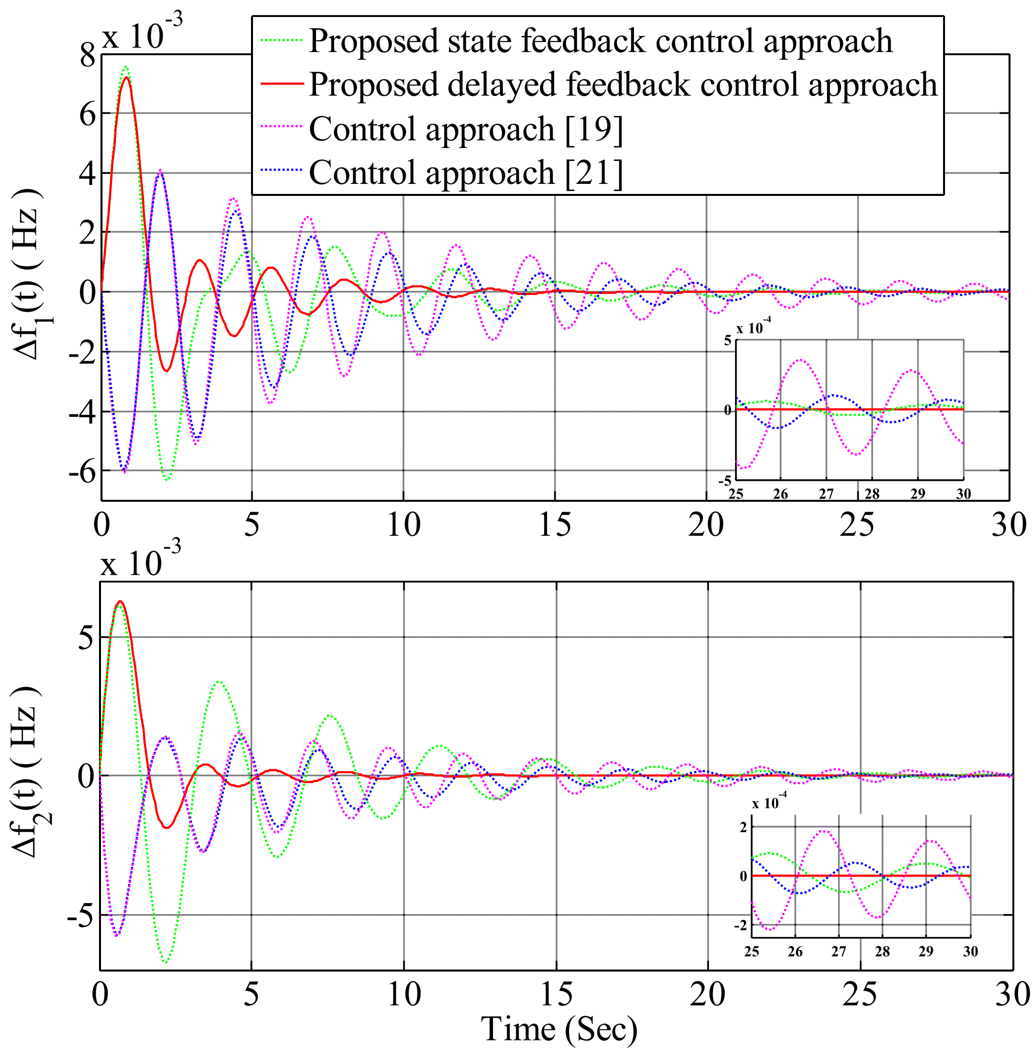

Fig. 7 Frequency deviations for step load change in the uncertain closed-loop IPS

$$K=\begin{bmatrix}-1.4381 & -0.0708 & -0.0256 & -0.0892 & 0.0860 & -13.3958 & -0.1344 & -0.0709 & -0.7348\\ -18.7202 & -0.2593 & -0.0540 & -0.6518 & -0.7116 & 40.1205 & 0.4610 & 0.4992 & 0.8281\end{bmatrix} \tag{46}$$

$$K=\begin{bmatrix}12.9569 & 0.1235 & 0.0090 & 0.9976 & 0.3836 & -46.6727 & -0.4983 & -0.3601 & -1.7016\\ -39.3775 & -0.6914 & -0.1782 & -1.8792 & -1.2455 & 81.3836 & 0.9720 & 1.1957 & 1.7138\end{bmatrix} \tag{47}$$

$$K_h=\begin{bmatrix}3.3359 & 0.0373 & 0.0049 & 0.2395 & 0.0957 & -10.8436 & -0.1175 & -0.0914 & -0.3812\\ -7.6956 & -0.1540 & -0.0439 & -0.3067 & -0.2435 & 11.8959 & 0.1536 & 0.2358 & 0.1204\end{bmatrix} \tag{48}$$

$$K=\begin{bmatrix}-1.2050 & -0.0611 & -0.0221 & -0.0587 & 0.0883 & -13.4954 & -0.1348 & -0.0773 & -0.7272\\ -18.9126 & -0.2665 & -0.0566 & -0.6697 & -0.7214 & 40.2924 & 0.4640 & 0.5123 & 0.8353\end{bmatrix} \tag{49}$$

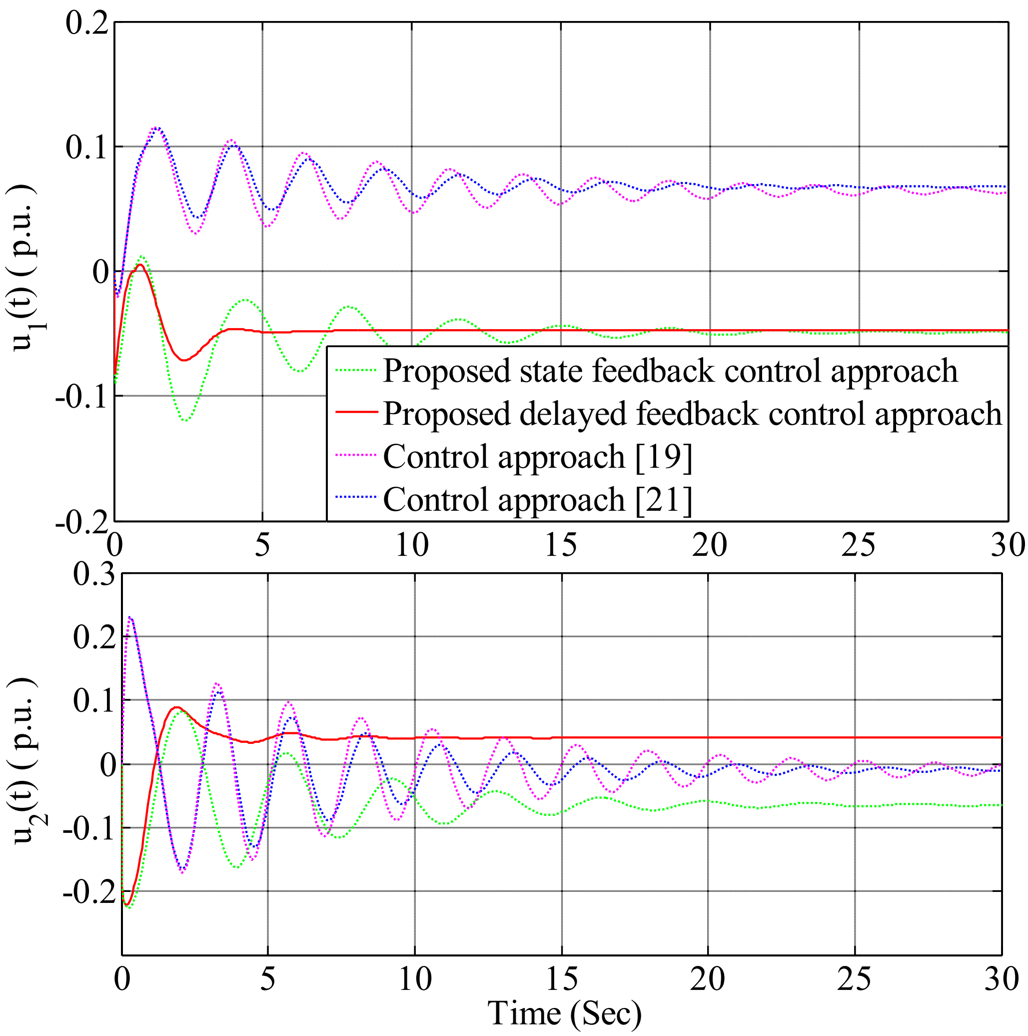

Fig. 8 Control inputs to the uncertain closed-loop IPS with step load change

$$K=\begin{bmatrix} 13.0885 & 0.1440 & 0.0111 & 1.0001 & 0.3854 & -47.5581 & -0.5056 & -0.3468 & -1.6900 \\ -40.3655 & -0.7169 & -0.1827 & -1.8897 & -1.2745 & 80.9309 & 1.0033 & 1.2113 & 1.7092 \end{bmatrix} \tag{50}$$

$$K_h=\begin{bmatrix} 3.3394 & 0.0380 & 0.0103 & 0.2510 & 0.1151 & -11.0578 & -0.1207 & -0.1124 & -0.3707 \\ -7.9684 & -0.1498 & -0.0492 & -0.3119 & -0.2342 & 12.1195 & 0.1651 & 0.2224 & 0.1192 \end{bmatrix} \tag{51}$$

In Table 2, a comparative study of h and γ values is presented. Larger h and smaller γ are obtained by using the proposed control approach in comparison to the other existing values [19, 21]. A larger value of σ indicates better delay tolerability of the closed-loop IPS [2], while a smaller value of γ indicates a better reduction of disturbance effect on the system performance [8]. As the existence of time-delay in LFC scheme of IPS is an inevitable phenomenon, improvement in delay tolerability improves the stability of the IPS. As load disturbance is the main cause of load frequency deviation in IPS, the reduction of disturbance effect on system performance results in better stability of IPS.

Next, simulation studies of the proposed LFC schemes are performed in MATLAB/Simulink using the above mentioned parameters of the two-area delayed IPS and the H_∞ performance-based sliding mode controllers. The

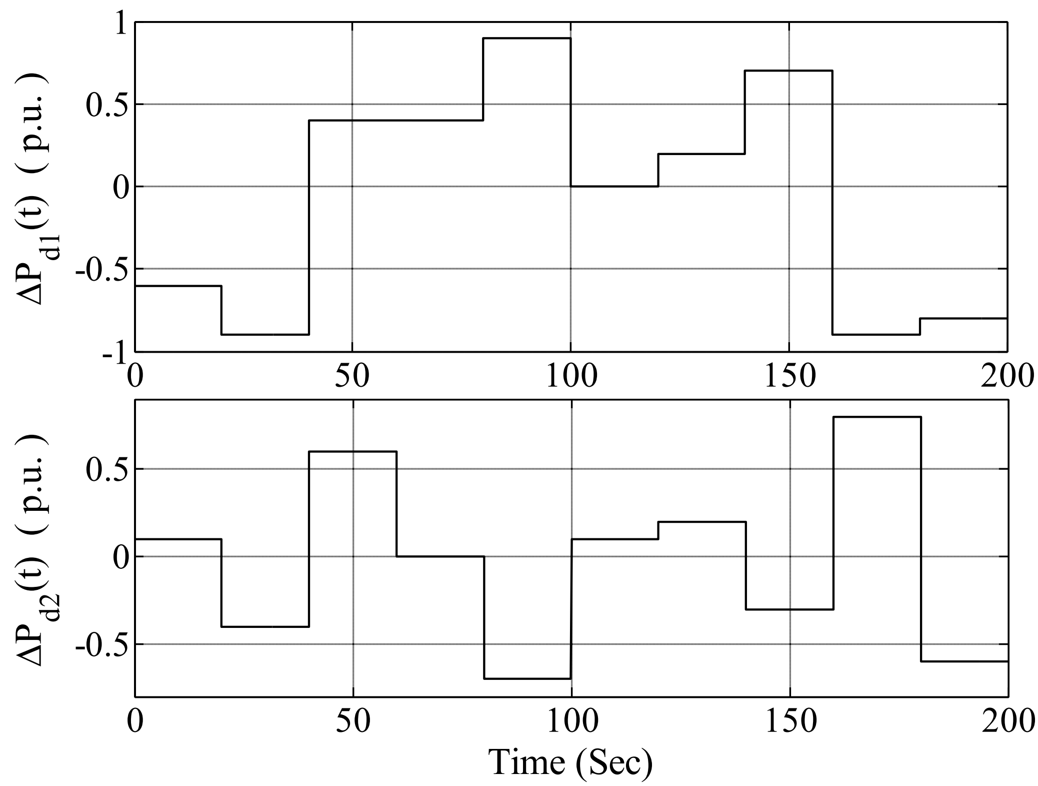

Fig. 9 Random load change in the two-area IPS

H_∞ state feedback sliding mode LFC model is shown in Fig. 3. As seen, the LFC model consists of the two-area delayed IPS and the proposed H_∞ state feedback sliding mode controller. In Fig. 3, w_1 and w_2 are the disturbances of area-1 and area-2, respectively, while $\sigma_1(t)$ and $\sigma_2(t)$ are the sliding mode switching surface functions for area-1 and area-2, respectively. u_1 and u_2 are the respective H_∞ state feedback SMC terms to area-1 and area-2. B_1 and D_1 are the first columns of the matrices B and D, respectively, while B_2 and D_2 are the second columns of the matrices B and D, respectively. J_1 and J_2 are the first and second rows of the matrix J, while K_1 and K_2 are the first and second rows of the controller gain matrix K, respectively.

Similarly, the H_∞ delayed feedback sliding mode LFC model is shown in Fig. 4. As shown, the LFC model consists of the two-area delayed IPS and the proposed H_∞ delayed feedback sliding mode controller. In Fig. 4, w_1 and w_2 are the disturbances of area-1 and area-2, respectively, $\sigma_1(t)$ and $\sigma_2(t)$ are the sliding mode switching surface functions for area-1 and area-2, respectively, and u_1 and u_2 are the H_∞ delayed feedback SMC terms to area-1 and area-2, respectively. B_1 and D_1 are the first columns of the matrices B and D, respectively, while B_2 and D_2 are the second columns of the matrices B and D, respectively. J_1 and J_2 are the first and second rows of the matrix J. K_1 and K_{h1} are the first rows of the controller gain matrices K and K_h, respectively, while K_2 and K_{h2} are the second rows of the controller gain matrices K and K_h, respectiv ely.

4.2 Simulation results

The two-area closed-loop delayed power system without parametric uncertainty [i.e., state-space model of two-area IPS (6) with SMC laws (35) and (45)], and the two-area closed-loop delayed power system with parametric uncertainty [i.e., state-space model of two-area IPS (8) with SMC laws (35) and (45)], are simulated in MATLAB/Simulink platform. Simulation studies on LFC schemes (i.e., state feedback H_∞ SMC and delayed feedback H_∞ SMC) are analyzed by considering step load disturbances and random load disturbances in both areas of the IPS.

In [19], a two-term H_∞ LFC scheme based on delayed feedback controller designing strategy is proposed for a two-area IPS with time-delay. Moreover, in [21], delayed feedback H_∞ LFC scheme is proposed for a two-area IPS with time-delay and parametric uncertainty. By using the two-area IPS parameters shown in Table 1, simulation studies of the schemes in [19] and [21] are performed in

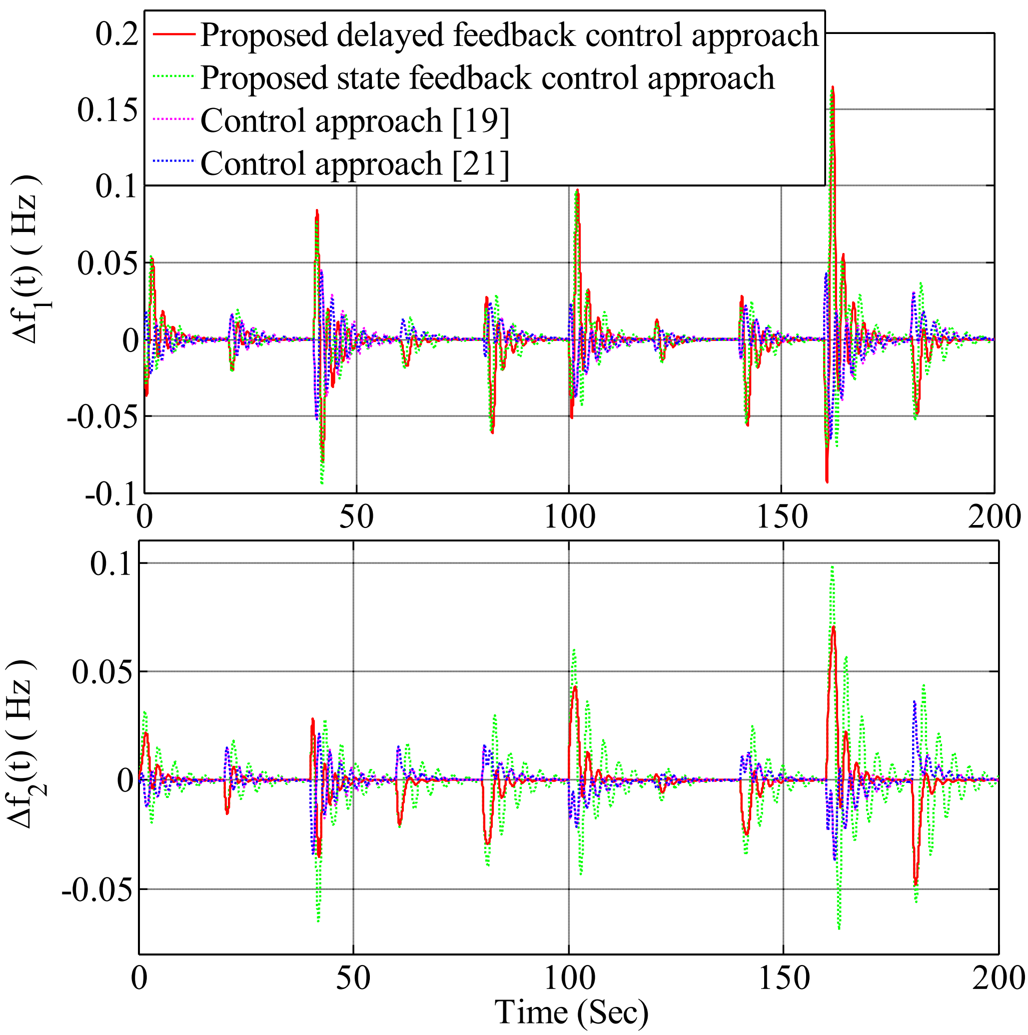

Fig. 10 Frequency deviations for random load change in the closed-loop IPS

MATLAB/Simulink for both step load disturbances and random load disturbances in the two areas of the IPS. The simulation results of the proposed LFC schemes and the LFC schemes of [19] and [21] are then compared.

4.2.1 Step-load disturbance

Step-load changes in control area-1 and control area-2 are set as $\Delta P_{d1} = 0.1$ p.u. and $\Delta P_{d2} = 0.2$ p.u., respectively. Simulation results on frequency deviations and control signals of the closed-loop IPS without parametric uncertainty are shown in Figs. 5 and 6, respectively. In comparison, the frequency deviations and control signals of the closed-loop IPS with parametric uncertainty are shown in Figs. 7 and 8, respectively.

It is observed from Figs. 5 and 7 that the frequency deviations of the two-area delayed IPS with and without parametric uncertainty are converging to zero within 15s by adopting the proposed delayed feedback H_∞ SMC law (45). In comparison, by adopting the proposed state feedback H_∞ SMC law (35) or the control approaches of [19, 21] (i.e., delayed feedback H_∞ control approaches), the frequency deviations of the two-area delayed IPS with and without parametric uncertainty take almost 30s for converging to zero. Furthermore, the observation of these frequency response curves in between 25 to 30 s is interesting, during which the frequency deviations of the two-area delayed IPS with and without parametric uncertainty are almost zero by using the proposed delayed feedback H_∞ SMC law (45). The damping of frequency deviation of the two-area delayed IPS without parametric uncertainty by using the proposed state feedback H_∞ SMC law (35) is not much better than those using the control approaches of [19, 21] (see Fig. 5), whereas, the damping of frequency deviation of the two-area delayed

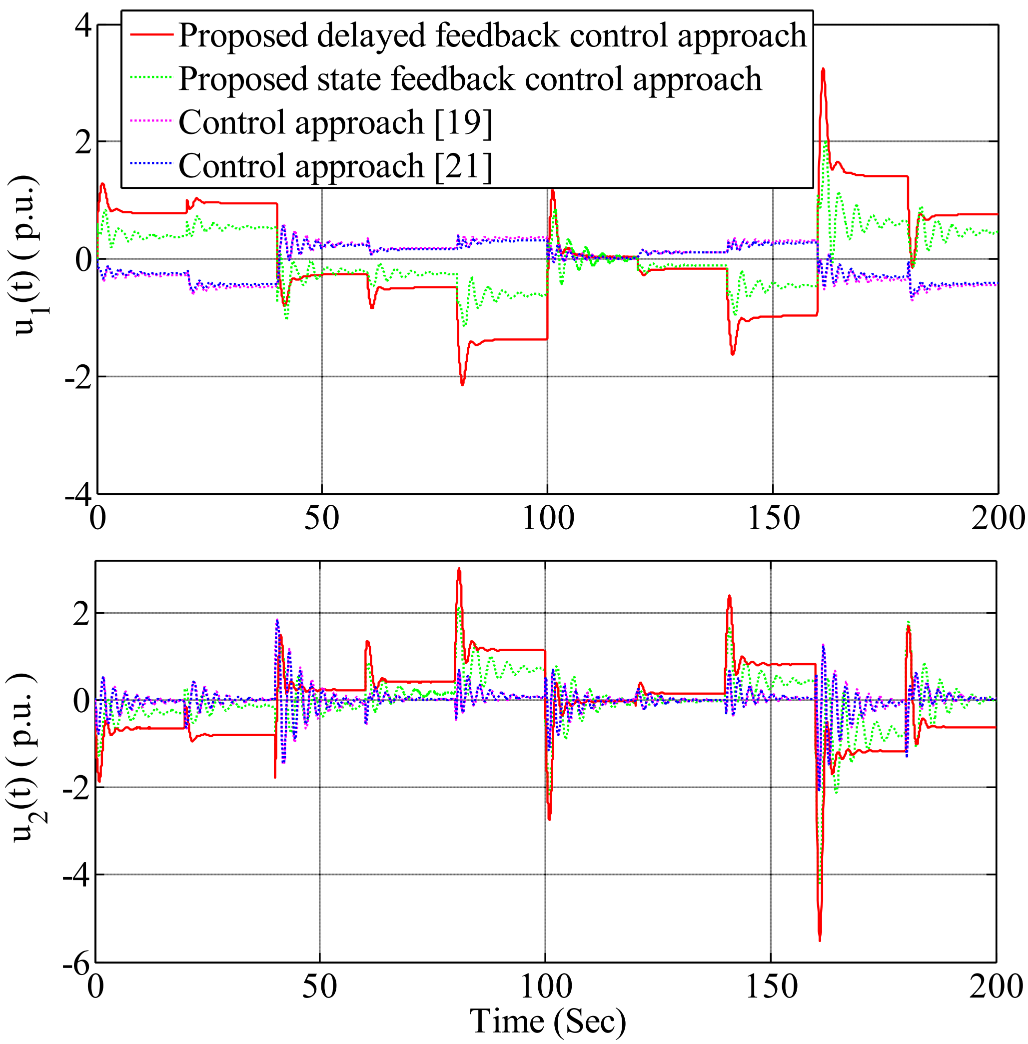

Fig. 11 Control inputs to the closed-loop IPS with random load change

IPS with parametric uncertainty by using the proposed state feedback H_∞ SMC law (35) is better than that of using the control approaches of [19, 21] (see Fig. 7). Therefore, by comparing the frequency response curves of Figs. 5 and 7 from 25*s* to 30*s*, one can observe that the proposed control approaches perform better than the existing control approaches for the consideration of parametric uncertainty in delayed IPS. There is not much difference in the respective frequency response curves of delayed IPS with and without parametric uncertainty by using the proposed approaches. This study shows that the proposed H_∞ performance-based sliding mode controllers are not sensitive to parametric variation.

One can observe from Fig. 6 that the convergence of control signals generated by the proposed delayed feedback H_∞ SMC law (45) for the two-area delayed IPS without parametric uncertainty is faster than the control signals generated by the proposed state feedback H_∞ SMC law (35) or the control approaches of [19, 21]. Also, From Fig. 8, one can observe that with consideration of parametric uncertainty in the delayed IPS, the convergence of control signals generated by both the proposed control approaches is faster than those generated by the control approaches of [19, 21]. Moreover, it can be observed from Figs. 6 and 8 that the control signals generated by the proposed methods are free from chattering. There are significant differences in the convergence values of control signals produced by the proposed H_∞ SMC laws (35) and (45), due to the difference in the structure of H_∞ SMC laws (35) and (45). The H_∞ SMC law (45) contains a delayed state feedback term, which is not present in the structure of the H_∞ SMC law (35).

The above analysis of the simulation results indicates that the performance of the proposed H_∞ SMC approaches is better than the performance of the existing H_∞ control approaches [19, 21] in terms of robustness

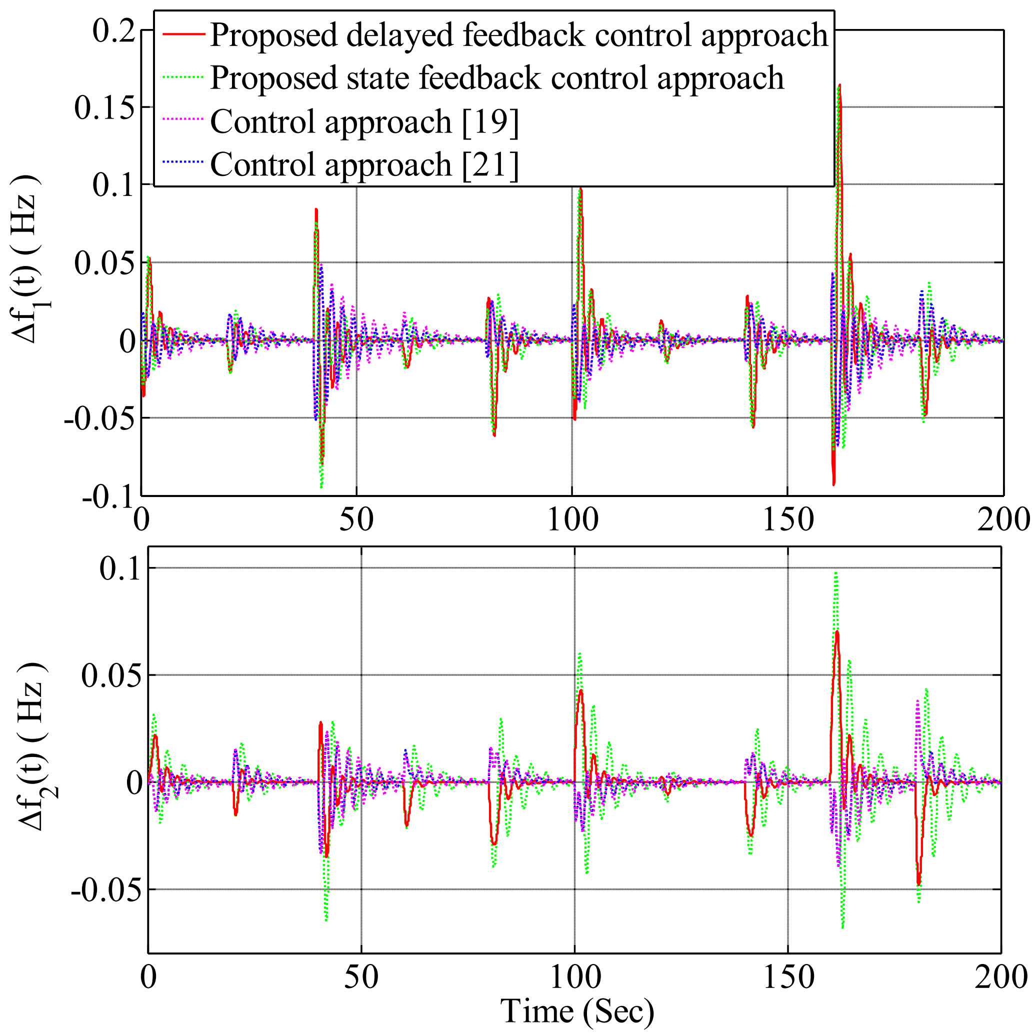

Fig. 12 Frequency deviations for random load change in the uncertain closed-loop IPS

against parametric uncertainty, fast convergence and disturbance rejection performance. Furthermore, better load frequency regulation of delayed IPS is obtained with the proposed delayed feedback H_∞ SMC approach than the proposed state feedback H_∞ SMC approach. This means that artificial delay incorporation in SMC structure improves stability of delayed power system.

4.2.2 Random-load disturbance

Random-load disturbances applied to control area-1 and control area-2 are shown in Fig. 9. Frequency deviations and control signals of the closed-loop delayed IPS without parametric uncertainty are depicted in Figs. 10 and 11, respectively. Considering uncertainty in the closed-loop delayed IPS parameters, frequency deviations and control signals are depicted in Figs. 12 and 13, respectively.

It is observed from Figs. 10 and 12, the proposed control schemes reduce frequency deviations of the delayed IPS satisfactorily for random-load changes. Damping of frequency deviations by using the delayed feedback H_∞ SMC strategy (45) is better than that of state feedback H_∞ SMC strategy (35). Moreover, from Figs. 11 and 13, one can observe that the control signals generated by the delayed feedback H_∞ SMC strategy (45) have faster convergence rate than those by the state feedback H_∞ SMC strategy (35). This observation shows that incorporation of artificial delay in SMC structure improves the stability of IPS with time-delay. The control signals [i.e., $u_1(t)$ and $u_2(t)$] generated by the proposed H_∞ SMC approaches for the delayed IPS areas are chattering free. Hence, H_∞ criterion based sliding mode controllers (35) and (45) give chattering free control signals. Furthermore, one can observe from these simulation results (i.e., Figs. 10, 11, 12 and 13) that the performance of the

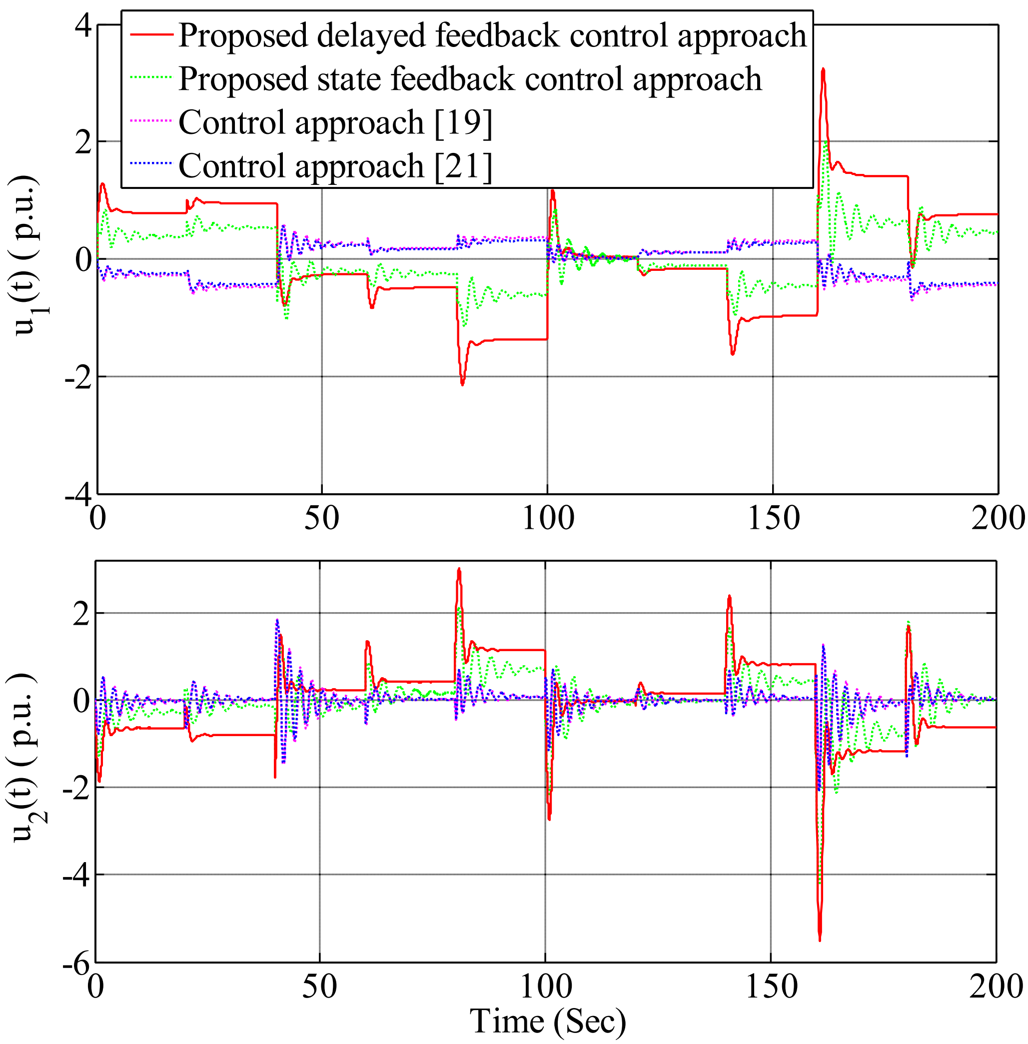

Fig. 13 Control inputs to the uncertain closed-loop IPS with random load change

proposed control approaches is better than the existing control approaches [19, 21] in terms of frequency regulation and control signal convergence of the closed-loop delayed IPS with random-load change in each control area.

The objective of any control design for load frequency regulation of IPS is to maintain any load frequency oscillation within acceptable range, which in power system is defined by two main levels such as statutory limit and operational limit [4]. Frequency oscillation of ± 0.5 Hz and ± 0.2 Hz are acceptable in statutory and operational limits, respectively [8]. From the frequency response curves shown in Figs. 5, 7, 10, and 12, it is clearly observed that frequency oscillations in each area of the closed-loop delayed IPS with and without parametric uncertainty are within the range of ± 0.2 Hz. This observation indicates that the load frequency oscillation of delayed IPS with and without parametric uncertainty is damped satisfactorily by using the proposed H_∞ performance-based sliding mode controllers. Hence, application of the proposed sliding mode H_∞ LFC designs based on the proposed state feedback control and delayed feedback control strategies can make IPS operation safe, secure and stable.

H_∞ performance-based state feedback sliding mode controller (35) and H_∞ performance-based delayed feedback sliding mode controller (45) take state variables of the state-space model (6) as their inputs and generate control signals for the two-area delayed IPS. Performance of controller (35) depends on the selection of suitable values of controller parameters b_1, b_2, J and K. Similarly, performance of controller (45) depends on the selection of suitable values of controller parameters b_1, b_2, h, J, K and K_h. The values of b_1 and b_2 are selected according to the disturbances of area-1 and area-2, respectively, while the value of h is tuned by considering the values of time-delays appeared in area-1 and area-2. Selection of matrix J depends on the input matrix B of the state-space model (6), while computation of K and K_h needs the values of τ_1, τ_2, h, and matrices A, A_{d1}, A_{d2}, B, C, D of the state-space model (6) and (2). The matrices A, A_{d1}, A_{d2}, B, C and D are obtained by using the values of the two-area IPS parameters given in Table 1. In real situation, the number of control areas of an IPS is not limited to two, and there may be a variety of generation technologies in each control area. For such situation, the number of state variables of the IPS (i.e., number of inputs to controller) and number of control inputs to IPS (i.e., number of controller outputs) may increase, which increase the dimensions of matrices A, A_{d1}, A_{d2}, B, C, D and J. Hence, dimensions of controller gain matrices K and K_h are increased and new values of K and K_h are computed. The above discussed changes in power system and controller parameters may change the control performance in real situations.

Conventional control design for load frequency regulation of IPS consists of an integral controller or a PI controller in each control area of the IPS to control the frequency oscillation of the respective control area [19]. Integral controllers and PI controllers are preferred to design conventional LFC schemes due to their simple structure and availability of various tuning methods [21], and when used in each control area of IPS for load frequency regulation, they are known as local controllers. For high and random load demand change as shown in Fig. 9, the local controllers may take a long time (up to several minutes) to bring the frequency oscillation to its tolerable limit. To handle such situation, the proposed sliding mode H_∞ LFC designs based on state feedback or delayed feedback control strategies can be considered, since in the proposed LFC designs, local controllers are considered as integral parts of the IPS while an H_∞ sliding mode controller is used to solve LFC problem of such IPS which already has local controllers. By observing the results analyzed in this paper, it is evident that the application of the proposed H_∞ performance-based sliding mode LFC designs can bring the frequency oscillation of IPS to its tolerable limit within a minute.

5 Conclusions

Two types of sliding mode controller designs are proposed in this paper by considering two different strategies, such as state feedback control strategy and delayed feedback control strategy, for power frequency regulation of delayed IPS with parametric uncertainty. In the delayed feedback sliding mode controller design, an artificial delay is incorporated intentionally to obtain better dynamic performance of the closed-loop delayed IPS. To obtain minimal disturbance effect on the performance of closed-loop systems (delayed IPS with state feedback sliding mode controller and with delayed feedback sliding mode controller), two delay-dependent H_∞ criteria (Theorems 1 and 3) in LMI framework are developed separately using two separate LK functionals for the stabilization of the two closed-loop IPSs with time-delay and parametric uncertainty. Stabilizing controller gains of these two types of sliding mode controllers are computed from the solution of these developed H_∞ criteria. These proposed LFC methods are tested for a numerical example of a two-area power system. Results of the test system show that these control methods can damp frequency deviations adequately for both step and random load changes in each control area. The findings of this paper are summarized as follows:

- The proposed H_∞ performance-based sliding mode controller designs for load frequency regulation of delayed IPS with parametric uncertainty are not affected by chattering. So, its control performance is improved.
- Damping of frequency oscillation is significantly improved by using the delayed feedback H_∞ SMC approach in comparison to the state feedback H_∞ SMC approach, which indicates that incorporation of an artificial delay in SMC design improves the stability of IPS with time-delay.
- For the high and random load changes in each area of the delayed IPS (see Fig. 9), the frequency oscillations are within the operational limit (± 0.2 Hz) by adopting the proposed H_∞ SMC approaches (see Figs. 10 and 12). This observation shows the applicability of the proposed control approaches for making the operation of IPS stable, secure and safe.
- The performance of the proposed delayed feedback H_∞ sliding mode LFC approach is superior to those of the existing delayed feedback H_∞ LFC approaches [19, 21] in terms of robustness against parametric variation, fast convergence and disturbance attenuation performance.

The study may be extended to analyzing the load frequency regulation of IPS considering a variety of generation technologies in each control area. Controller design for load frequency regulation of time-delay IPS with parametric uncertainty may also be proposed by using fractional order sliding mode controller in place of the integral sliding mode controller.

Appendix A Proof of Theorem 2

Consider the Lyapunov function as:

$$V(t) = \frac{1}{2}\sigma^T(t)\sigma(t). \tag{52}$$

Derivative of (52) is given by:

$$\dot{V}(t) = \frac{1}{2}\dot{\sigma}^T(t)\sigma(t) + \frac{1}{2}\sigma^T(t)\dot{\sigma}(t) = \sigma^T(t)\dot{\sigma}(t). \tag{53}$$

Using (13), one can write (53) as:

$$\dot{V}(t) = \sum_{i=1}^{2}\sigma_i(t)\{J_iB_iK_ix(t) + J_iB_iu_i(t) + J_iD_iw_i(t)\}. \tag{54}$$

Substituting (35) in (54), one obtains:

$$\dot{V}(t) = \sum_{i=1}^{2}\sigma_i(t)\left[-b_i\|J_iD_i\|\left(\frac{\sigma_i(t)}{\|\sigma_i(t)\| + \zeta}\right) + J_iD_iw_i(t)\right]. \tag{55}$$

Equation (55) can be expressed as:

$$\dot{V}(t) \leq \sum_{i=1}^{2}[-b_i\|J_iD_i\|\|\sigma_i(t)\| + \|\sigma_i(t)\|\|J_iD_i\|\|w_i(t)\|]. \tag{56}$$

The above equation may be further solved as:

$$\dot{V}(t) \leq \sum_{i=1}^{2}\|\sigma_i(t)\|\|J_iD_i\|[-b_i + \|w_i(t)\|] < 0. \tag{57}$$

Thus, control law (35) ensures $\sigma_i(t)\dot{\sigma}_i(t) < 0$.

Abbreviations

SMC	Sliding mode control
IPS	Interconnected power system
LFC	Load frequency control
PI	Proportional-integral
PID	Proportional-integral-derivative
LMI	Linear matrix inequality
LK	Lyapunov–Krasovskii
ACE	Area control error

List of symbols

ΔP_{vi}	Governor valve position deviation of area *i*
ΔP_{mi}	Mechanical output power deviation of area *i*
Δf_i	Frequency deviation of area *i*
ΔP_{ij}	Tie-line power deviation of area *i* and area *j*
ΔP_{di}	Load disturbance of area *i*
T_{gi}	Governor time constant of area *i*
T_{pi}	Power system time constant of area *i*
T_{chi}	Turbine time constant of area *i*
T_1	Stiffness coefficient between area 1 and area 2
k_{pi}	Power system gain of area *i*
k_i	Gain of local integral controller of area *i*
ΔE_i	Output of local integral controller in area *i*
B_i	Frequency bias parameter of area *i*
R_i	Speed droop of area *i*
τ_i	Time-delay in control area *i*
h	Artificial delay
u_i	Control input to area *i*
K	Controller gains correspond to present states
K_h	Controller gains correspond to delayed states
γ	H_∞ performance index
I	Identity matrix with proper dimension
R^{-1}	Inverse of matrix *R*
R^T	Transpose of matrix *R*
*	Symmetric terms of a matrix

Acknowledgements
Not applicable.

Author contributions
SKP: Writing—original draft, conceptualization, validation, methodology, formal analysis. DKDas: Supervision, resources, writing—reviewing and editing.

Funding
Not applicable.

Availability of data and materials
Not applicable.

Declarations

Competing interests
The authors declare that they have no known competing financial interests or personal relationships that could have appeared to influence the work reported in this paper.

Received: 13 November 2022 Accepted: 5 September 2023
Published online: 07 October 2023

References

1. Ahmed, M., Magdy, G., Khamies, M., & Kamel, S. (2022). Modified TID controller for load frequency control of a two-area interconnected diverse-unit power system. *International Journal of Electrical Power & Energy Systems, 135*, 107528.
2. Pradhan, S. K., & Das, D. K. (2020). H_∞ load frequency control design based on delay discretization approach for interconnected power systems with time delay. *Journal of Modern Power Systems and Clean Energy, 96*, 1468.
3. Guo, J. (2021). Application of a novel adaptive sliding mode control method to the load frequency control. *European Journal of Control, 57*, 172–178.
4. Pradhan, S. K., & Das, D. K. (2022). Delay-discretization-based sliding mode H_∞ load frequency control scheme considering actuator saturation of wind-integrated power system. *The Journal of Supercomputing, 78*, 1–46.
5. Chen, P., Zhang, D., Yu, L., & Yan, H. (2022). Dynamic event-triggered output feedback control for load frequency control in power systems with multiple cyber attacks. *IEEE Transactions on Systems, Man, and Cybernetics: Systems, 52*, 6246.
6. Sun, Y., Wang, Y., Wei, Z., Sun, G., & Wu, X. (2018). Robust H_∞ load frequency control of multi-area power system with time delay: a sliding mode control approach. *IEEE/CAA Journal of Automatica Sinica, 5*(2), 610–617.
7. Pradhan, S. K., Das, D. K. (2019). H_∞ performance based robust state feedback controller design for interconnected power system with delay. In *2019 2nd international conference on innovations in electronics, signal processing and communication (IESC)*, (pp. 263–268). IEEE.
8. Pradhan, S. K., & Das, D. K. (2022). H_∞ controller design for frequency control of delayed power system with actuator saturation and wind source integration. *Arabian Journal for Science and Engineering, 47*, 1–19.
9. Su, X., Liu, X., & Song, Y.-D. (2017). Event-triggered sliding-mode control for multi-area power systems. *IEEE Transactions on Industrial Electronics, 64*(8), 6732–6741.

10. Li, M., & Chen, Y. (2018). A wide-area dynamic damping controller based on robust H_∞ control for wide-area power systems with random delay and packet dropout. *IEEE Transactions on Power Systems, 33*(4), 4026–4037.
11. Pradhan, S. K., Das, D. K. (2021). Inter-area oscillation damping considering time-varying communication delay of wide-area power system. In *2021 international symposium of asian control association on intelligent robotics and industrial automation* (IRIA), (pp. 154–159). IEEE.
12. Pradhan, S. K., Das, D. K. (2019). Development of H_∞ based static state feedback controller for interconnected power system with time-delay using sector bounding actuator saturation approach. In *2019 international conference on electrical, electronics and computer engineering (UPCON)*, (pp. 1–6). IEEE.
13. Sheirah, M., & Abd-El-Fattah, M. (1984). Improved load-frequency self-tuning regulator. *International Journal of Control, 39*(1), 143–158.
14. Toulabi, M., Shiroei, M., & Ranjbar, A. (2014). Robust analysis and design of power system load frequency control using the Kharitonov's theorem. *International Journal of Electrical Power & Energy Systems, 55*, 51–58.
15. Lim, K., Wang, Y., & Zhou, R. (1996). Robust decentralised load-frequency control of multi-area power systems. *IEE Proceedings-Generation, Transmission and Distribution, 143*(5), 377–386.
16. Zribi, M., Al-Rashed, M., & Alrifai, M. (2005). Adaptive decentralized load frequency control of multi-area power systems. *International Journal of Electrical Power & Energy Systems, 27*(8), 575–583.
17. Dong, L., Zhang, Y., & Gao, Z. (2012). A robust decentralized load frequency controller for interconnected power systems. *ISA Transactions, 51*(3), 410–419.
18. Sivaramakrlshnan, A., Hariharan, M., & Srisailam, M. (1984). Design of variable-structure load-frequency controller using pole assignment technique. *International Journal of control, 40*(3), 487–498.
19. Dey, R., Ghosh, S., Ray, G., & Rakshit, A. (2012). H_∞ load frequency control of interconnected power systems with communication delays. *International Journal of Electrical Power & Energy Systems, 42*(1), 672–684.
20. Xiong, L., Li, H., & Wang, J. (2018). LMI based robust load frequency control for time delayed power system via delay margin estimation. *International Journal of Electrical Power & Energy Systems, 100*, 91–103.
21. Zhao, X., Sun, Y., Li, N., Wei, Z., Sun, G., & Huang, C. (2016). Robust H_∞ load frequency control of delayed multi-area power system with stochastic disturbances. *Neurocomputing, 32*, 4110.
22. Bevrani, H., & Hiyama, T. (2008). Robust decentralised PI based LFC design for time delay power systems. *Energy Conversion and Management, 49*(2), 193–204.
23. Yu, X., & Tomsovic, K. (2004). Application of linear matrix inequalities for load frequency control with communication delays. *IEEE Transactions on Power Systems, 19*(3), 1508–1515.
24. Bevrani, H., Mitani, Y., & Tsuji, K. (2004). Robust decentralised load-frequency control using an iterative linear matrix inequalities algorithm. *IEE Proceedings-Generation, Transmission and Distribution, 151*(3), 347–354.
25. Jiang, L., Yao, W., Wu, Q., Wen, J., & Cheng, S. (2012). Delay-dependent stability for load frequency control with constant and time-varying delays. *IEEE Transactions on Power systems, 27*(2), 932–941.
26. Zhang, C.-K., Jiang, L., Wu, Q., He, Y., & Wu, M. (2013). Delay-dependent robust load frequency control for time delay power systems. *IEEE Transactions on Power Systems, 28*(3), 2192–2201.
27. Yang, F., He, J., & Wang, D. (2017). New stability criteria of delayed load frequency control systems via infinite-series-based inequality. *IEEE Transactions on Industrial Informatics, 14*(1), 231–240.
28. Abdallah, C. T., Sipahi, R., Niculescu, S.-J., Michiels, W., & Gu, K. (2011). Stability and stabilization of systems with time delay: Limitations and opportunities. *IEEE Transactions on Control Systems Technology, 31*(1), 38.
29. Huschto, T., Feichtinger, G., Hartl, R. F., Kort, P. M., Sager, S., & Seidl, A. (2011). Numerical solution of a conspicuous consumption model with constant control delay. *Automatica, 47*(9), 1868–1877.
30. Shtessel, Y., Edwards, C., Fridman, L., & Levant, A. (2014). *Sliding mode control and observation*. New York: Springer.
31. Prasad, S., Purwar, S., & Kishor, N. (2016). H_∞ based non-linear sliding mode controller for frequency regulation in interconnected power systems with constant and time-varying delays. *IET Generation, Transmission & Distribution, 10*(11), 2771–2784.
32. Mi, Y., Hao, X., Liu, Y., Fu, Y., Wang, C., Wang, P., & Loh, P. C. (2017). Sliding mode load frequency control for multi-area time-delay power system with wind power integration. *IET Generation, Transmission & Distribution, 11*(18), 4644–4653.
33. Pradhan, S. K., & Das, D. K. (2021). H_∞ performance-based sliding mode control approach for load frequency control of interconnected power system with time delay. *Arabian Journal for Science and Engineering, 46*(2), 1369–1382.
34. Onyeka, A. E., Xing-Gang, Y., Mao, Z., Jiang, B., & Zhang, Q. (2020). Robust decentralised load frequency control for interconnected time delay power systems using sliding mode techniques. *IET Control Theory & Applications, 14*(3), 470–480.
35. Chen, P., Yu, L., & Zhang, D. (2020). Event-triggered sliding mode control of power systems with communication delay and sensor faults. *IEEE Transactions on Circuits and Systems I: Regular Papers, 68*(2), 797–807.
36. Azmi, H., & Yazdizadeh, A. (2022). Adaptive delay dependent sliding mode fault-tolerant controller design for nonlinear systems with unknown time-varying input and state delays. *European Journal of Control, 69*, 100756.
37. Kuppusamy, S., & Joo, Y. H. (2022). Dynamic integral sliding mode control for interconnected delayed power systems. *Journal of the Franklin Institute, 359*(16), 8742–8757.
38. Das, D. K. (2015). *New results on delay-dependent stability analysis and stabilization of time-delay systems*. PhD thesis
39. Kumar, A., Pradhan, S. K., Das, D. K. (2019) H_∞ performance based state feedback controller design for wind integrated interconnected power system with time-delay. In *2019 international conference on electrical, electronics and computer engineering (UPCON)*, (pp. 1–6). IEEE.
40. Das, D. K., Ghosh, S., & Subudhi, B. (2015). An improved robust stability analysis for systems with two delays by extracting overlapping feature. *Journal of Control and Decision, 2*(2), 124–141.
41. Boyd, S., El Ghaoui, L., Feron, E., Balakrishnan, V. (1994). *Linear matrix inequalities in system and control theory*, (pp. 1–193). SIAM.

Subrat Kumar Pradhan received the B. Tech. degree in Electrical Engineering in 2012 and the M. Tech. degree in Power System Engineering in 2016 from Biju Patnaik University of Technology, Odisha, India. He received the Ph.D. degree in Electrical and Electronics Engineering in 2022 from National Institute of Technology Nagaland, India. Since 2022, he has been with Indira Gandhi Institute of Technology, Sarang, Odisha, India as an Assistant Professor. His research interest includes the development of load frequency controllers for time-delay power systems using H-infinity control and sliding mode control techniques.

Dushmanta Kumar Das is a Member of IEEE. He received the B. Tech. degree in Electronics and Instrumentation Engineering from Biju Patnaik University of Technology, Odisha, India. He received the M. Tech. and the Ph.D. degrees in Control System Engineering from National Institute of Technology Rourkela, India in 2010 and 2015, respectively. Since 2013, he has been with National Institute of Technology Nagaland, India as an Associate Professor. His research interests include time-delay system, control system, robotics, soft computing, machine learning, meta-heuristic optimization techniques and application of optimization techniques.